Reviews

Gas-phase kinetic and theoretical studies of reactions of germylenes and dimethylstannylene

S. E. Boganov,[a] M. P. Egorov,[a]★ V. I. Faustov,[a] I. V. Krylova,[a] O. M. Nefedov,[a] R. Becerra,[b] and R. Walsh[c]★

[a]*N.D. Zelinsky Institute of Organic Chemistry, Russian Academy of Sciences, 47 Leninsky Prospekt, 119991 Moscow, Russian Federation*
Fax: +7 (095) 135 5328. E-mail: mpe@ioc.ac.ru
[b]*Instituto de Quimica-Fisica "Rocasolano", C.S.I.C., C/Serrano 119, 28006 Madrid, Spain*
Fax: + 34 (91) 5642431. E-mail: r.becerra@iqfr.csic.es
[c]*Department of Chemistry, University of Reading, Whiteknights, P.O. Box 224, Reading RG6 6AD, UK*
Fax: + 44 (0)118 3786331. E-mail: r.walsh@reading.ac.uk

The results of time-resolved gas phase studies of labile germylenes (GeH_2 and $GeMe_2$) and dimethylstannylene ($SnMe_2$) reactions reported to date are considered together with data of quantum-chemical investigations of the potential energy surfaces of these systems. Reaction mechanisms are discussed. A comparison of reactivity in the series of carbene analogs, ER_2 (E = Si, Ge, Sn, R = H, Me), is made.

Key words: germylene, dimethylgermylene, dimethylstannylene, reaction kinetics, time-resolved studies, quantum-chemical calculations, RRKM calculations, Arrhenius parameters, thermochemistry.

Introduction

Labile carbene analogs of the Group 14 elements, ER_2 (E = Si, Ge, Sn, Pb), are important intermediates of organoelement chemistry.[1] Despite a large number of publications[2—7] concerning their reactivities and physicochemical properties, the mechanisms of most of their reactions remain poorly understood. Very important quantitative information about reactivities and reaction mechanisms of these species can be obtained from kinetic studies. In the past two decades, the kinetics of many characteristic reactions of silylenes have been explored in detail.[8—10] The first absolute rate constants for germylene reactions were measured in the liquid phase at room temperature using the laser flash photolysis technique for $GeMe_2$,[11—19] $GeEt_2$,[19] $GeBu_2$,[19] $GeHex_2$,[19] GeMePh,[12,14,15,19] $GePh_2$,[12,14,15,20] and $GeMes_2$.[21] These studies revealed a surprising dependence of the absorption maximum of $GeMe_2$ and the rate constants for its reactions on the precursor used, which may be explained by the strong inclination of germylenes to form complexes with Lewis bases such as the solvent employed (or even the precursor).[7,22] Thus, kinetic measurements are best carried out in the gas-phase to eliminate these prob-

Published in Russian in *Izvestiya Akademii Nauk. Seriya Khimicheskaya,* No. 3, pp. 477—505, March, 2005.
1066-5285/05/5403-0483

lems and to try to reveal the true nature of the reactivities of germylenes (and indeed all carbene analogs). In this connection about ten years ago we started systematic direct time-resolved studies of the reaction kinetics of germylenes in the gas phase. The present review is devoted to the results obtained in this field by us and other research groups since that time. A special section of this review is devoted to the first results of the gas phase kinetic studies of $SnMe_2$ reactions, which represent the first kinetic data on reactions of any labile stannylene.

1. Kinetics and mechanisms of germylene reactions

1.1. Experimental techniques, precursors, detection, and identification of transient species

To date, gas-phase kinetic studies of germylenes have been focussed on prototype reactions of germylene itself, GeH_2, and of its simplest organic congener, dimethylgermylene, $GeMe_2$. The experimental technique used was laser flash photolysis. The apparatus required for this time-resolved method consisted of an optical reaction cell connected to a vacuum system for preparation of reaction mixtures, a photolysis laser, a probe laser and fast data recording and processing systems.[10,23—25] The reaction mixtures were made up of a precursor (in small concentrations), a substrate, and a bath gas (SF_6 or, in some experiments, N_2). Reactions were studied under pseudo-first-order conditions, with the substrate in excess over germylene. The concentration of the substrate was changed systematically from one experiment to another. The target second-order rate constant for the reaction under study was obtained from the dependence of the observed first-order decay constant for the transient species in question on the substrate concentration. The bath gas determined the total pressure in the reaction system, which was usually maintained in the range 1—100 Torr. This pressure range was limited by practical considerations. Above *ca.* 100 Torr, the signals of the transient species became too weak to be measured reliably, and below 1 Torr, pressure measurement uncertainties became significant. In the studies of the temperature dependence of the rate constants, the series of experiments described above was repeated at different temperatures (usually, five) between room temperature and the highest temperature allowed by the stabilities of either the precursor or the substrate.

Under experimental conditions (transient decay constants of *ca.* 10^4 s^{-1}, substrate pressures of 10^{-3}—10^2 Torr) the second-order rate constants in the range 10^{-10}—10^{-15} cm^3 $molecule^{-1}$ s^{-1} can be measured. These correspond to fast reactions with the rates ranging from 1 to 10^{-5} of the collision rate. This allows a rough estimate to be made of the upper limit of activation barrier, E_a, of 20—30 kJ mol^{-1}, above which reactions would be too slow to be studied by this experimental technique. We shall refer to these systems (carbene analogs plus a substrate) as non-reactive. It is important to note that the substrate purity can be very important because carbene analogs are, in general, highly reactive species, and in the case of a less reactive substrate, the reaction may occur with any impurities present.

Dimethylgermylene, $GeMe_2$, is one of the simplest organogermylenes. It plays an important role in the chemistry of organogermanium compounds.[4,5] It was our first target.[25]

We used pentamethyldigermane (PMDG) as the photoprecursor of $GeMe_2$ for time-resolved studies. In preliminary experiments, a second precursor, 1,1-dimethyl-1-germacyclopent-3-ene (GCP), was also used to validate the identity of the observed transient species as $GeMe_2$.[25] Besides, tetramethyldigermane, $HMe_2GeGeMe_2H$ was also found to be a good precursor of $GeMe_2$.[26]

Silicon analogs of these compounds are known to be good photochemical sources of $SiMe_2$ in the gas phase.[10,25,27] Moreover, GCP is known to produce $GeMe_2$ upon thermolysis,[28—30] a usually reliable indicator. Thus, both PMDG and GCP seemed obvious candidates as precursors of $GeMe_2$.

PMDG and GCP show strong UV absorptions (λ_{max} = 202 nm, extinction coefficient = $2.5 \cdot 10^3$ dm^3 mol^{-1} cm^{-1} and λ_{max} = 190 nm, extinction coefficient = $2.1 \cdot 10^3$ dm^3 mol^{-1} cm^{-1}, respectively),[25] making them suited to photolysis studies at 193 nm, the main operating wavelength of the photolysis laser (ArF exciplex) used in these studies.

End product analysis revealed that Me_3GeH and buta-1,3-diene are the major stable products of photolysis of PMDG and GCP at 193 nm:[25]

$$Me_3GeGeMe_2H \xrightarrow{i} Me_3GeH + GeMe_2 \quad (1)$$

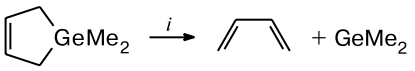

(2)

i. *h*ν, 193 nm.

In addition, photolysis of PMDG in presence of buta-1,3-diene resulted in the formation of GCP,[25] the product of $GeMe_2$ trapping with buta-1,3-diene:

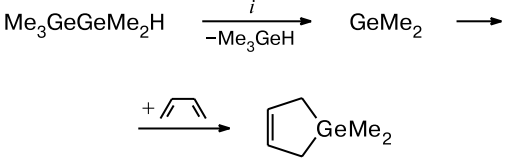

(3)

i. *h*ν, 193 nm.

All these facts imply that the decompositions of PMDG and GCP upon photolysis at 193 nm produce $GeMe_2$ as the major transient species.

Under time-resolved conditions transient absorption spectra were obtained in the 450–510 nm region for each precursor.[25] These spectra were broad band with maxima at the same wavelength of 476.5 nm, although under the same photolysis conditions and precursor concentrations the absorption recorded using PMDG was 1.5 times as intense as that using GCP. Decay constants measured for these absorptions were independent of the probe wavelength in the whole spectral region. This indicates that both compounds produce the same transient species absorbing in this wavelength region.[25] This region is characteristic of the $^1B_1 \leftarrow {}^1A_1$ electronic transition of germylenes,[7] and particularly for $GeMe_2$, whose UV absorption was earlier recorded in both the liquid phase and low-temperature matrices,[7] but never before in the gas phase. Because photolysis of GCP was accompanied by dust formation, making work with this precursor difficult, all the kinetic studies discussed below were performed using PMDG as precursor.

Germylene, GeH_2, is a progenitor of the germylene series. It is a species important in the chemical vapor deposition (CVD) of semiconductor germanium,[31–33] and is a key intermediate in the breakdown mechanism of germanium hydrides.[34] In the time-resolved studies, GeH_2 was generated by photodecomposition of 3,4-dimethylgermacyclopent-3-ene (DMGCP)[23] or phenylgermane, $PhGeH_3$,[23,24] although several experiments were also carried out using $MesGeH_3$.[35] Phenylgermane is a known photochemical source of GeH_2.[36–38] By analogy with this source and also with the precursors of dimethylgermylene, $MesGeH_3$ and DMGCP were also tested as precursors of GeH_2.

Phenylgermane and DMGCP show strong UV absorptions ($\lambda_{max} = 205$ nm, extinction coefficient $= 2.6 \cdot 10^3$ $dm^3\ mol^{-1}\ cm^{-1}$ and $\lambda_{max} = 198$ nm, extinction coefficient $= 3.2 \cdot 10^3$ $dm^3\ mol^{-1}\ cm^{-1}$),[23] making them suited to photolysis studies at 193 nm. The main stable gaseous products upon photolysis of these precursors at 193 nm were found to be benzene and 2,3-dimethylbuta-1,3-diene, respectively:[23]

$$PhGeH_3 \xrightarrow{i} PhH + GeH_2, \qquad (4)$$

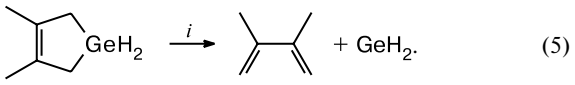

(5)

i. *h*ν, 193 nm.

Calibration showed that yield of benzene corresponds to 20±2 % of decomposed $PhGeH_3$. Photolysis of $PhGeH_3$ in the presence of oxygen (in large excess) reduced conversion, but the yield of benzene with respect to the converted precursor was almost unchanged.[23] This strongly argues against involvement of free radicals in the process of GeH_2 formation. Substantial gas-borne dust formation accompanied photolysis of $PhGeH_3$, which made this precursor inconvenient for kinetic studies. However, it was shown later[24] that by use of special precautions $PhGeH_3$ could successfully be used as a precursor in kinetic measurements (see below).

The yield of 2,3-dimethylbuta-1,3-diene from DMGCP was more than 70 %, implying that the formation of GeH_2 is the major process in the 193 nm photolysis of DMGCP. Besides, photodecomposition of DMGCP did not give concomitant dust formation. In a trapping experiment similar to that for $GeMe_2$, photolysis of $PhGeH_3$ at 193 nm in the presence of a great excess of 2,3-dimethylbuta-1,3-diene resulted in DMGCP [23]:

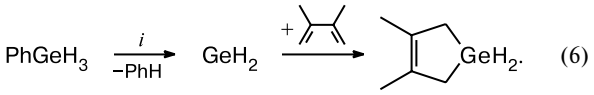

(6)

i. *h*ν, 193 nm.

A search for intense GeH_2 rovibronic lines suitable for kinetic measurements was carried out for both precursors in the wavenumber ranges 17109.28 – 17113.10 and 17116.68 – 17120.00 cm^{-1}. These regions were chosen based on the published fluorescence spectra of GeH_2 [36–39] recorded in a cooled molecular jet (where the effective temperature was *ca*. 20 K and only lines corresponding to low rotational quantum numbers were observed). The spectra revealed that the band origin of the most intense $^1B_1(0,1,0) \leftarrow {}^1A_1(0,0,0)$ transition occurs at 17108.516 cm^{-1}.[36–39] As a result, a fragment of the room-temperature spectrum of GeH_2 was obtained from two different precursors.[23] Later, the complete spectrum of GeH_2 at room temperature was recorded using intra-cavity laser absorption spectroscopy,[40] and all the features of the GeH_2 spectrum detected in the kinetic study[23] were confirmed. The strong rovibronic line at 17111.31 cm^{-1}, corresponding to the $^{74}GeH_2$ isotopomer, was mainly used in the kinetic measurements considered below, although in some experiments this isotopomer was also monitored by following its transition at 17118.67 cm^{-1} in order to verify that the results were independent of the wavelength. Study of the photochemistry of the third precursor, $MesGeH_3$, was limited to detection of the strong absorption signals at 17111.31 and 17118.67 cm^{-1} upon its laser photolysis at 193 nm, clearly indicating the formation of GeH_2:[35]

$$MesGeH_3 \xrightarrow{i} MesH + GeH_2. \qquad (7)$$

i. *h*ν, 193 nm.

1.2. First absolute rate constants for GeH_2 and $GeMe_2$ reactions in the gas phase at room temperature

The first measured absolute rate constants for GeH_2 reactions at room temperature[23] are collected in Table 1. The uncertainties shown are single standard deviations.

Table 1. Gas-phase rate constants (k) for reactions of GeH_2 at room temperature at a total pressure of 10 Torr

Substrate	$k \cdot 10^{10}$/cm^3 molecule^{-1} s^{-1}			
	DMGCP[a] 193 nm[23]	$PhGeH_3$[a,b,c]		$MesGeH_3$[b] 193 nm[35]
		193 nm[24]	248 nm[24]	
O_2	$(6.11\pm0.17)\cdot10^{-3}$	—	—	—
C_2H_2	1.29±0.04	1.38±0.04	—	—
i-C_4H_8	1.24±0.08	1.41±0.10	1.21±0.05	—
1,3-C_4H_6	3.03±0.12	—	—	3.4±0.2
C_3H_8	$<1.1\cdot10^{-4}$ [d]	—	—	—
Me_2GeH_2	2.38±0.11[b,e]	—	—	—
Me_3SiH	$(8.18\pm0.14)\cdot10^{-1}$	1.03±0.05	0.92±0.11	$(8.65\pm0.38)\cdot10^{-1}$
DMGCP	3.48±0.16	—	—	—
$PhGeH_3$	—	3.00±0.10	—	—

[a] N_2 as a bath gas.
[b] SF_6 as a bath gas.
[c] The rate constants are independent of pressure in the range 10—50 Torr.
[d] $PhGeH_3$ was used as a precursor.
[e] Data taken from Ref. 26 (SF_6 as a bath gas).

The kinetic measurements were carried out upon production of GeH_2 from DMGCP by photolysis at 193 nm in N_2 buffer gas at 10 Torr total pressure. The results show that GeH_2 readily adds to π-bonds of unsaturated organic compounds and inserts into Si—H and Ge—H bonds although not into C—H bonds. The lack of reaction of GeH_2 with propane at room temperature on the time scale of the experiments allowed setting an upper limit to the rate constant. Kinetic experiments carried out in SF_6 with another precursor, $MesGeH_3$, for two substrates, Me_3SiH and buta-1,3-diene,[35] showed good agreement with the data obtained using DMGCP as the precursor (Table 1). However, when we generated GeH_2 from $PhGeH_3$, the measured rate constants appeared significantly lower than those obtained using DMGCP and $MesGeH_3$.[23] It was especially puzzling, because both $MesGeH_3$ and $PhGeH_3$ are structurally similar aromatic compounds.[23] The photolysis of $PhGeH_3$ was accompanied by strong dust formation and the decay traces were noisy. Thus, the values obtained with the use of DMGCP (and $MesGeH_3$) seemed more reliable. Although a possible explanation for the surprising decrease in the rate constants was suggested,[23] it was later demonstrated that $PhGeH_3$ could be used for kinetic measurements under appropriate experimental conditions, which include the use of a flow reaction cell and background subtraction from the recorded decay trace.[24] The rate constants measured by Alexander *et al.*[24] under such conditions with $PhGeH_3$ as the precursor coincided within experimental error with those obtained by us using DMGCP as the precursor[23] (Table 1), confirming that the latter are correct. Besides, the authors[24] photolyzed $PhGeH_3$ at the two wavelengths of 193 and 248 nm, which led to the same values of the rate constants. This strongly supports the fact that vibrational relaxation is complete under experimental conditions and has no effect on the kinetic measurements.

The room-temperature rate constants for reactions of $GeMe_2$ in the gas phase are collected in Table 2.[25] They were obtained using PMDG as the $GeMe_2$ precursor and SF_6 as the bath gas. $GeMe_2$ was monitored at 476.5 nm, near its gas-phase absorption maximum. Substrates were chosen to cover a selection of potential reaction types. No reaction was found with C_3H_8 (33 Torr), Me_3SiH (112 Torr) or Me_3GeH (2.5 Torr),[25] although later the reaction with Me_2GeH_2 was observed[26] (see the next section). However, reactions with oxygen, 3,3-dimethylbut-1-ene, acetylene, and buta-1,3-diene did occur. For the unreactive substrates, the lack of reaction was used to set upper limits for the rate constants.

The gas-phase rate constants for reactions of $GeMe_2$ may be compared with those measured in solution. Selected solution rate constants are also listed in Table 2. The differences are rather striking, although direct comparisons are only possible for buta-1,3-diene and O_2. It is noteworthy that, where more than one precursor has been used, the solution data are in mutual disagreement, as seen for the reactions of $GeMe_2$ with buta-1,3-diene and Et_3SiH. This was also true for the reaction of $GeMe_2$ with CCl_4,[17,18] a substrate not investigated in the gas phase because of its photolysis at 193 nm. These discrepancies were attributed to complexation with the aromatic π-system when arylated precursors were used.[18] Probably, this is one of the main factors causing the significant scatter in solution rate constant values. However, this suggestion does not explain the difference in rate constants obtained

Table 2. Room-temperature rate constants (k) for reactions of $GeMe_2$

Substrate	k/cm^3 molecule^{-1} s^{-1} (p/Torr)	Reference
	Gas phase (SF_6 as a bath gas)	
O_2	$(4.5\pm0.3)\cdot10^{-14}$ [a]	25
C_2H_2	$(1.3\pm0.3)\cdot10^{-11}$ (3—30)	25
C_2H_4	$(8.9\pm0.8)\cdot10^{-13}$ (3)	25
	$(1.7\pm0.1)\cdot10^{-12}$ (10)	25
	$(4.0\pm0.3)\cdot10^{-12}$ (30)	25
	$(6.9\pm0.5)\cdot10^{-12}$ (100)	25
$H_2C{=}CHCMe_3$	$(9.9\pm0.6)\cdot10^{-12}$ (10, 30)	25
	$(1.3\pm0.3)\cdot10^{-11}$ (100)	25
1,3-C_4H_6	$(1.1\pm0.1)\cdot10^{-11}$ [a]	25
C_3H_8	$<2\cdot10^{-14}$	25
Me_3SiH	$<6\cdot10^{-15}$	25
Me_3GeH	$<4\cdot10^{-13}$	25
Me_2GeH_2	$(2.3\pm0.1)\cdot10^{-13}$ [a]	26
	$<9.3\cdot10^{-15}$	[b]
	Cyclohexane solution[c]	
O_2	$3.3\cdot10^{-12}$	16
1-C_4H_8	$<1.7\cdot10^{-16}$	16
1-C_6H_{12}	$<1.7\cdot10^{-17}$	16
1,3-C_4H_6	$2.8\cdot10^{-14}$	16
	$4.0\cdot10^{-14}$	14, 17
	$2.5\cdot10^{-12}$	18
Et_3SiH	$<1.7\cdot10^{-17}$	16
	$7.0\cdot10^{-15}$	14, 15

[a] Pressure independent.
[b] R. Becerra, M. P. Egorov, I. V. Krylova, O. M. Nefedov, and R. Walsh; unpublished results.
[c] $GeMe_2$ was generated from $(PhMe_2Ge)_2GeMe_2$,[14,15] $PhMe_2GeSiMe_3$,[16] *cyclo*-$(Me_2Ge)_6$,[17] and *cyclo*-$(Me_2Ge)_5$.[18]

when $GeMe_2$ was produced from *cyclo*-$(Me_2Ge)_6$ and *cyclo*-$(Me_2Ge)_5$,[17,18] and also disagreements between the gas-phase rate constants and solution rate constants measured using non-aromatic precursors. It is worth noting that the absorption maxima of the transient species observed in the course of solution kinetic measurements were quite varied: 420,[14,15] 425,[16] 450,[17] and 490 [18] nm, which implies the presence of some other factors affecting the germylene in solution. Therefore, the gas-phase rate constants seem to be the most reliable. Some of the confusions over the solution studies have been clarified only recently.[41]

The gas-phase rate constants obtained allow comparison of the reactivity of silylenes and germylenes on a quantitative basis. The data presented in Table 3 show that GeH_2 is slightly less reactive than SiH_2 (usually, by factors of 2—4), but in general displays the same pattern of reactivity. Both species readily react with alkenes and alkynes, but are unreactive toward alkanes, both easily insert into Si—H bonds and slowly interact with oxygen. Methyl substituents reduce the reactivity of both germylene and silylene through inductive electron withdrawal. $GeMe_2$ is somewhat less reactive than $SiMe_2$.

Table 3. Comparison of gas-phase rate constants (k) for reactions of SiH_2, GeH_2, $SiMe_2$, and $GeMe_2$ at room temperature[a]

Substrate	k/cm^3 molecule^{-1} s^{-1}			
	SiH_2 [10]	GeH_2 [23]	$SiMe_2$ [10]	$GeMe_2$ [25]
O_2	$>1.4\cdot10^{-11}$	$6.1\cdot10^{-13}$	$2.5\cdot10^{-13}$	$4.5\cdot10^{-14}$
C_2H_2	$3.2\cdot10^{-10}$	$1.3\cdot10^{-10}$	$4.6\cdot10^{-11}$	$1.3\cdot10^{-11}$
Alkene[b]	$3.6\cdot10^{-10}$	$1.2\cdot10^{-10}$	$3.7\cdot10^{-11}$	$1.3\cdot10^{-11}$
1,3-C_4H_6	$>1.9\cdot10^{-10}$	$3.0\cdot10^{-10}$	$7.5\cdot10^{-11}$	$1.1\cdot10^{-11}$
Alkane[c]	$<1.7\cdot10^{-13}$	$<1.1\cdot10^{-14}$	$<5\cdot10^{-14}$	$<2\cdot10^{-14}$
Me_3SiH	$2.5\cdot10^{-10}$	$8.2\cdot10^{-11}$	$4.5\cdot10^{-12}$	$<6\cdot10^{-15}$

[a] For known pressure-dependent reactions, the high-pressure limiting values are listed.
[b] C_3H_6 (SiH_2, $SiMe_2$), *i*-C_4H_8 (GeH_2), and $Me_3CCH{=}CH_2$ ($GeMe_2$).
[c] Me_4Si (SiH_2, $SiMe_2$) and C_3H_8 (GeH_2, $GeMe_2$).

1.3. Insertion into σ-bonds

Insertion into σ-bonds is one of the characteristic reactions of heavy carbene analogs.[2—5,9,10] Insertion reactions of the heavy methylene analogs, SiH_2 and GeH_2, into Si—H and Ge—H bonds, respectively, are important processes in the breakdown mechanisms of silanes and germanes which lead to chemical vapor deposition of electronically useful materials.[42,43] Product studies show that GeH_2 readily inserts into both Ge—H and Si—H bonds.[44,45] Relative rate measurements for reactions of GeH_2 with Ge_2H_6, methylgermanes, Me_nGeH_{4-n} (n = 1—3), and Me_3SiH at 280 °C suggest it to be a fairly reactive but discriminating species.[46] This work represents the only published relative rate study of the GeH_2 insertion process.

Preliminary gas-phase kinetic studies[23,24] also showed that GeH_2 easily inserts into the Si—H bond of Me_3SiH and the Ge—H bond of $PhGeH_3$. Interaction of GeH_2 with DMGCP[23] is a very fast process, but it is not clear whether it represents a Ge—H insertion or a C=C addition process. In contrast, $GeMe_2$ was found[25] to be rather unreactive toward Ge—H and Si—H bonds of Alk_3EH (E = Si, Ge; see Tables 1 and 2, respectively), although there is evidence[28] that $GeMe_2$ inserts into a Ge—H bond.

Later, the reaction of $GeMe_2$ (monitored at 488 nm) with Me_2GeH_2 was observed[26] (but see below and Table 2). The choice of substrate was made by analogy with the $SiMe_2$ + Me_2SiH_2 system, which showed the greatest rate constants among the $SiMe_2$ + Me_nSiH_{4-n} (n = 0—3) reaction systems.[10] The room-temperature rate constant for the interaction of GeH_2 with Me_2GeH_2 was also measured for comparison (Table 1).[26] Both reactions were supposed not to be pressure dependent by analogy with the SiH_2 + Me_2SiH_2 reaction.[10] For the $GeMe_2$ + Me_2GeH_2 reaction, the lack of a pressure dependence was indicated by the fact that the total pressure

varied (depending on the concentration of Me_2GeH_2) during the experiments and no curvature in the second-order plot (dependence of transient first-order decay constant, k_{obs}, on the pressure of Me_2GeH_2) was found. The results obtained showed a dramatic rate decrease (by a factor of 1050) for $GeMe_2$ relative to GeH_2 in this insertion reaction. More recent observations suggest (see Table 2) that the rate decrease may be even greater.[47] The decrease in reactivity on going from SiH_2 to $SiMe_2$ in the analogous reaction with Me_2SiH_2 is much smaller, *ca*. by a factor of 60.[48,49] Thus, methyl-for-H substitution is much more deactivating for germylene than for silylene. The reasons for this deactivating effect will be discussed below.

Now we will discuss the prototype GeH_2 and $GeMe_2$ insertion processes, for which the kinetics have been studied in detail.

Systems GeH_2 + EH_4 (E = Ge, Si). Reaction (8) of germylene with monogermane may reasonably be considered a prototype Ge—H insertion process in germanium hydride chemistry. It occurs when GeH_2 is formed *via* recoil Ge atoms generated in the neutron bombardment of GeH_4,[44] and is the likely final step in any process leading to the generation of Ge_2H_6 from GeH_4. The kinetics of this reaction have not been investigated previously.

The absolute rate constants for the reactions (8) [35] and (9) [50] were measured over a wide temperature range and at different total pressures (SF_6), as is listed in Table 4, using DMGCP as precursor

$$GeH_2 + GeH_4 \longrightarrow Ge_2H_6 \qquad (8)$$

$$GeH_2 + SiH_4 \longrightarrow H_3GeSiH_3 \qquad (9)$$

It was found that the rate constants decrease with an increase in temperature at all pressures. Such a behavior often implies the reaction mechanism to involve reversible formation of an intermediate complex lying in energy below the initial reagents.[57] At a given temperature, the rate constants increase with an increase in pressure, the extent of variation being the largest at the highest temperature. Although the pressure dependences tend toward high-pressure limiting values at each temperature, this is actually approached only at room temperature. These effects are characteristic of third-body assisted association reactions.

Modeling of the pressure dependence by RRKM calculations of the reverse unimolecular reactions (–8) and (–9), whose pressure dependence should correspond exactly to those of reactions (8) and (9) respectively, providing there are no other perturbing reaction channels, gave good fits to the experimental data at each temperature and allowed extrapolation to infinite pressure. The high-pressure rate constants thus obtained gave the Arrhenius parameters for both reactions (they are also listed in Table 4). These parameters provide evidence for moderately fast reactions occurring at approximately one-fifth (reaction 8) and one-twenty fifth (reaction 9) of the collision rate.[50] Slowing down of the reactions with an increase in temperature is reflected in the negative values of their activation energies. Other outcomes of the RRKM modeling are the values of the critical (Marcus) energy, E_0, of the reverse reactions (–8) and (–9) not reported before. The E_0 values were used to derive the heat of formation and Divalent State Stabilization Energy (DSSE) of germylene (see below).

$$Ge_2H_6 \longrightarrow GeH_2 + GeH_4, \qquad (-8)$$

$$H_3SiGeH_3 \longrightarrow GeH_2 + SiH_4. \qquad (-9)$$

The kinetic parameters of the GeH_2 reactions (8) and (9) resemble those of the SiH_2 insertion reactions (10) [54] and (11) [55] listed in Table 4 for comparison.

Table 4. Arrhenius parameters and high-pressure limiting rate constants for GeH_2 insertion reactions and the corresponding reactions of SiH_2

Reaction	T/K	p/Torr	$-\log A$	$-E_a$	E_0(reverse)	k^∞ (T/K)	Reference
				kJ mol^{-1}			
$GeH_2 + GeH_4 \rightarrow Ge_2H_6$	292—520	1—100	11.17±0.10	5.2±0.7	155±12	$(5.5\pm0.6)\cdot10^{-11}$ (292)	35
$GeH_2 + SiH_4 \rightarrow H_3GeSiH_3$	295—554	1—100	11.73±0.06	4.6±0.4	138±12	$(1.3\pm0.1)\cdot10^{-11}$ (295)	50
$GeH_2 + Et_3GeH \rightarrow Et_3GeGeH_3$	292—557	1—100[a]	11.43±0.15	10.6±1.1	—	$(2.7\pm0.1)\cdot10^{-10}$ (292)	51
$GeH_2 + Me_3SiH \rightarrow Me_3SiGeH_3$	295—528	1—100[a]	12.15±0.06	11.6±0.4	—	$(8.2\pm0.1)\cdot10^{-11}$ (295)	52
	295—436	10[b]	11.8±0.1	11.0±0.4	—	$(1.03\pm0.05)\cdot10^{-10}$ (295)	53
$GeH_2 + PhGeH_3 \rightarrow PhGeH_2GeH_3$	295—436	10[b]	10.1±0.1	3.6±0.3	—	$(3.0\pm0.1)\cdot10^{-10}$ (295)	53
$SiH_2 + SiH_4 \rightarrow Si_2H_6$	298—665	1—100	9.91±0.04	3.3±0.3	216.7	$(4.6\pm0.3)\cdot10^{-10}$ (296)	54
$SiH_2 + GeH_4 \rightarrow H_3SiGeH_3$	295—553	1—100[a]	9.88±0.02	2.1±0.2	—	$(3.1\pm0.1)\cdot10^{-10}$ (295)	55
$SiH_2 + Me_3SiH \rightarrow Me_3SiSiH_3$	295—625	3—100[a]	10.11±0.05	2.9±0.3	—	$(2.5\pm0.1)\cdot10^{-10}$ (298)	10, 56

Note: the A and k^∞ values are given in cm^3 molecule^{-1} s^{-1}.

[a] There is no pressure dependence.

[b] No pressure dependence was assumed at all temperatures based on the absence of the dependence at room temperature.[24]

$$SiH_2 + SiH_4 \longrightarrow Si_2H_6 \quad (10)$$

$$SiH_2 + GeH_4 \longrightarrow H_3SiGeH_3 \quad (11)$$

The mechanisms of SiH_2 insertion processes have been considered in detail in a recent review.[10] As can be seen from Table 4, reactions (8) and (9) are characterized by lower rates and hence lower collision efficiencies compared to their SiH_2 analogs. This is reflected in lower A factors for the GeH_2 insertions. The estimated[35,50] A factors for the decomposition of Ge_2H_6 and H_3GeSiH_3 according to equations (–8) and (–9) are *ca.* $10^{14.5}$ s^{-1} and *ca.* $10^{13.7}$ s^{-1}, respectively, whereas the corresponding value for Si_2H_6 decomposition is *ca.* $10^{16.0}$ s^{-1}.[54] Thus, the transition states for the reaction pathways of GeH_2 with EH_4 (E = Si, Ge) are significantly tighter than that for the reaction of SiH_2 with SiH_4. It is worth noting that the estimated A factors for all these decomposition reactions decrease slightly with an increase in temperature. Although this decrease is only slightly larger than the uncertainty of the estimates, it is consistent with the variational behavior of the transition states of the processes.

All these findings can be understood in terms of a mechanism *via* an intermediate complex, established earlier for SiH_2 insertion processes[10] and supported for GeH_2 reactions (8) and (9) by *ab initio* and DFT calculations[35,50] (Scheme 1).

Scheme 1

$$EH_2 + E'H_4 \underset{k_{-1}}{\overset{k_1}{\rightleftharpoons}} H_2E\cdots H^*\text{—}E'H_3 \longrightarrow$$

$$\longrightarrow TS^{\#} \xrightarrow{k_2} H_3EE'H_3$$

E, E′ = Si, Ge

Quantum-chemical calculations of the systems GeH_2 + GeH_4 and GeH_2 + SiH_4. Quantum-chemical calculations at the MP2/6-311G(d,p) level showed[35] the presence of five stationary points on the Ge_2H_6 potential energy surface (PES) in addition to those of the reactants, GeH_2 + GeH_4, and the product, Ge_2H_6. These correspond to two local minima, **C1** and **C2**, and three transition states, **TS0**, **TS1**, and **TS2**, which are shown in Fig. 1. The minima represent H-bridged weakly bound complexes with *syn*- (**C1**) and *anti*- (**C2**) configuration of the GeH_2 moiety relative to the Ge—H bond that is formed. The existence of such complexes was evidenced in earlier *ab initio* calculations at the lower SCF/ECP level of theory.[58] Each complex has an associated transition state, **TS1** and **TS2**, linking it to digermane.[35] The passage *via* **C1** and **TS1** to digermane involves an inversion of configuration of the GeH_3 group that is formed, while that *via* **C2** does not. Complex **C1** has a C_1 symmetry and exists as left- (**C1**(l)) and right-handed (**C1**(r)) forms, which are separated by a very low-lying transition state **TS0**. Similarly, **TS2** possessing C_1 symmetry is represented by left- (**TS2**(l)) and right-handed (**TS2**(r)) forms separated by a low rotational maximum. Such departure from the more symmetrical C_s to C_1 structure for the complex **C1** was not found in the previous calculations,[58] but was found for related Sn_2H_6 and Pb_2H_6 species.[58] The reason for the lowering of symmetry for **TS2** and complexes like **C1** is obscure.

Similar stationary points **C1**, **C2**, **TS0**, **TS1**, and **TS2**, with left- and right-handed forms for **C1** and **TS2**, were found on the PES of the GeH_2 + SiH_4 system in quantum-chemical calculations at the *ab initio* MP2/6-311G(d,p) and DFT B3LYP/6-311++G(3df,2pd) levels.[50] Both methods gave good agreement on their geometries.

The topology diagram in Fig. 2 shows pathways through the stationary points found, starting from GeH_2 + EH_4 up to H_3EGeH_3 (E = Si, Ge). Omitting the complexity resulting from the existence of right- and left-handed enantiomeric species, the pathways of the reactions (8) and (9) are in close resemblance to those over the Si_2H_6 potential energy surface revealed earlier from *ab initio* calculations at the MP2/6-311G(d,p) level of theory.[54] The most prominent differences between these systems are as follows. In the complexes **C1** and **C2** formed in the reactions (8) and (9), the migrating hydrogen atom (H*) is closer to the E atom of EH_4 than the Ge atom of germylene. Indeed, for the GeH_2 + GeH_4 system at the MP2 level,[35] the Ge—H* distances are 1.603 and 1.862 Å for **C1**, 1.573 and 1.981 Å for **C2**, and for the GeH_2 + SiH_4 system at the MP2 (B3LYP) level,[50] the Ge—H* distances are 1.898 (1.877) and 1.971 (1.963) Å for **C1** and **C2**, respectively, whereas the Si—H* distances are 1.527 (1.540) and 1.510 (1.520) Å for **C1** and **C2**, respectively. This suggests that the H-atom transfer is not very pronounced in either GeH_2 complex. In the complex **C1** (SiH_2 + SiH_4 system), there is a reverse situation, the migrating atom H* is closer to the Si atom of silylene. The Si—H* distances are 2.046 (from the Si atom of silane) and 1.525 Å (from the Si atom of silylene),[54] thus showing a much more significant H-transfer. However, complex **C2** in the SiH_2 + SiH_4 system is characterized by much smaller degree of H-atom transfer (the corresponding Si—H* distances are[54] 1.548 and 1.760 Å) and it is therefore more akin to the corresponding complexes in the GeH_2 reactions.

The energies associated with the stationary point species of the Ge_2H_6, $SiGeH_6$, and Si_2H_6 potential energy surfaces[35,50,54] are listed in Table 5. The **C1** + **TS1** pathway is seen to be energetically favored over **C2** + **TS2** for all the systems, although the latter looks more like the intuitively expected approach. In contrast to the SiH_2 reaction, the energy differences between the two complexes, **C1** and **C2**, are quite small for GeH_2 insertions. However, the barrier **TS2** is significantly higher than **TS1**

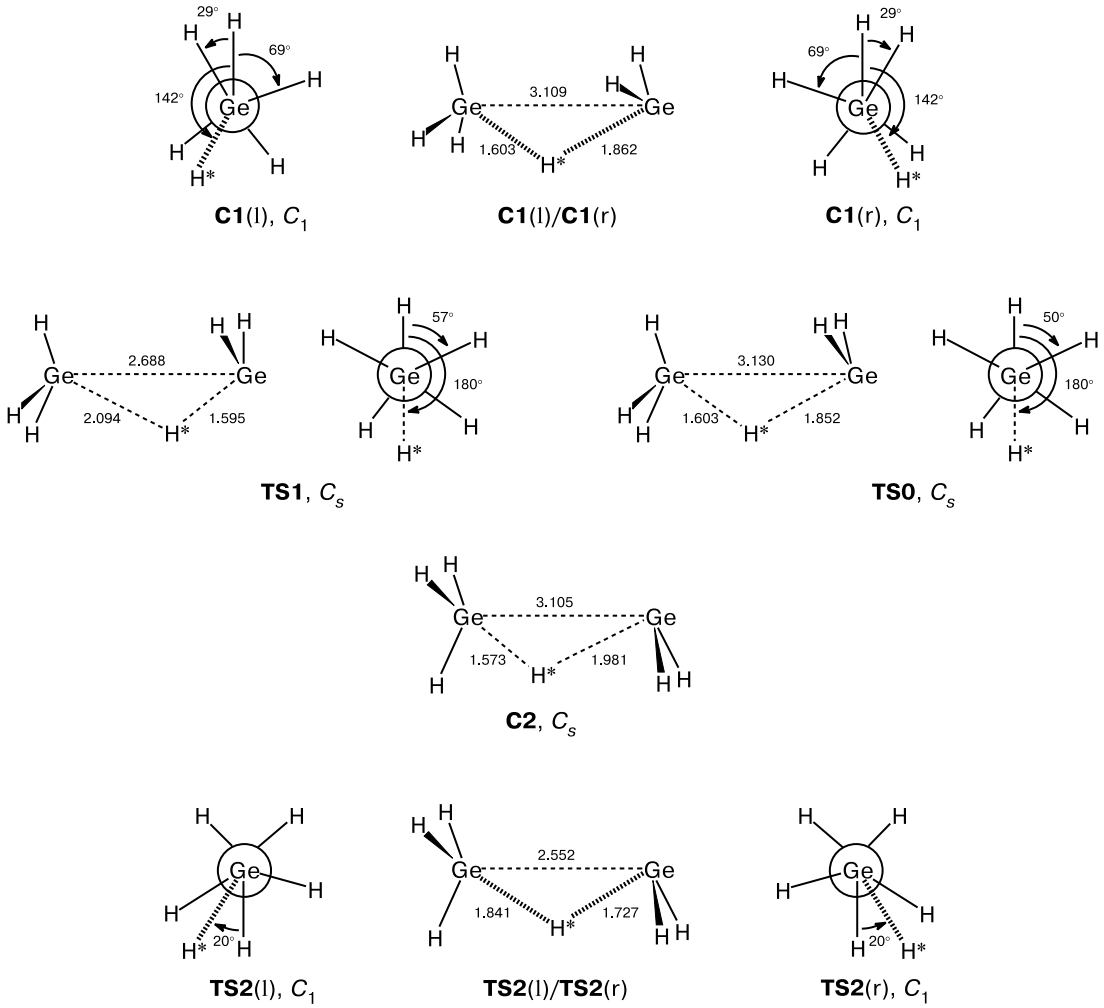

Fig. 1. Structures corresponding to local minima and transition states on the PES of the Ge_2H_6 system located in *ab initio* MP2/6-311G(d,p) calculations. The point symmetry groups are given beside the structure labels. The migrating H atom is asterisked.

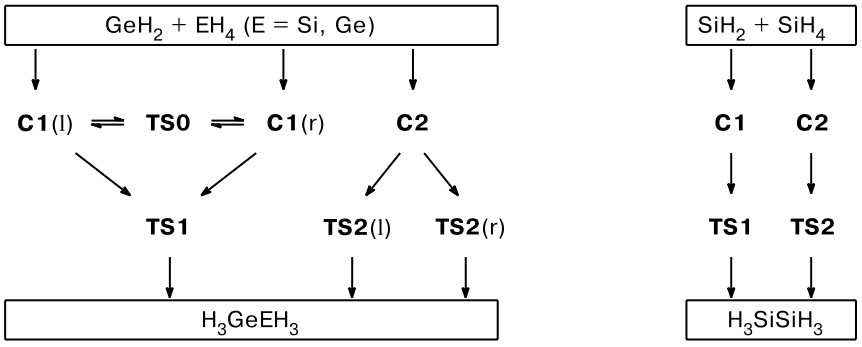

Fig. 2. Topology diagram of reactions $GeH_2 + EH_4$ (E = Ge, Si) and $SiH_2 + SiH_4$.

in the case of germylene, which suggests that for germylene insertions the pathway *via* **C2** is probably not operative. Indeed, the energy of **TS2** is somewhat higher than that of the starting $GeH_2 + GeH_4$ and only slightly lower than that of the starting reactants according to the G2 calculations. It is also worth noting that, in the B3LYP calculations of the $GeH_2 + SiH_4$ system, **TS1** and **TS2** lie in energy above the initial reagents (Table 5). The G2 data for this system are in better agreement with the experiment.

Table 5. Energies[a] (ΔE or ΔE + ZPE/kJ mol^{-1}) of the stationary points of the systems $EH_2 + E'H_4 \rightarrow H_3EE'H_3$ (E, E′ = Si, Ge) obtained from quantum-chemical calculations

State	$SiH_2 + SiH_4$ [54]	$GeH_2 + SiH_4$ [50]		$GeH_2 + GeH_4$ [35]	
	MP2/6-311G(d,p)	B3LYP/6-311++G(3df,2pd)	G2//MP2/6-311G(d,p)	MP2/6-311G(d,p)	G2//MP2/6-311G(d,p)
	ΔE	ΔE + ZPE	ΔE + ZPE	ΔE + ZPE	ΔE+ ZPE
$H_3EE'H_3$	−236.0	−145.4	−149.4	−178.9	−176.7
C1	−51.5	−19.3	−25.0	−23.0	−25.3
TS0	—[b]	−18.8	−23.8	−22.7	−24.9
TS1	−48.5	6.8	−5.0	−13.8	−16.6
C2	~−34[c]	−14.9	−21.5	−17.4	−19.6
TS2	~−34[c]	8.9	−0.7	−7.3	0.7

[a] Relative to the sum of the total energies of isolated molecules EH_2 and $E'H_4$.
[b] No stationary point was located.
[c] The authors[54] did not present the exact value, but gave some hints to it.

A comparison of the figures in Table 5 shows that H-bridged complexes in the case of GeH_2 are less thermodynamically stable relative to the initial reagents and more stable compared to the final products. The increase in stability of H-bridged structures such as **C1** relative to the stable E_2H_6 as the atomic number of E in Group 14 of the Periodic Table increases has already been demonstrated.[58] At the same time, the GeH_2 complexes are less prone to rearrangement to the insertion products than their SiH_2 analogs to Si_2H_6: the barrier heights are 10–20 kJ mol^{-1} for the GeH_2 complexes and *ca.* 0 kJ mol^{-1} for the SiH_2 complexes. However, in general both pathways of all the systems under consideration possess low barriers to rearrangement of the complexes to the final insertion products.

The overall changes in enthalpy at 298 K were calculated to be −180.6 kJ mol^{-1} (MP2) for reaction (8) and −153.9 (MP2) and −149.7 (B3LYP) kJ mol^{-1} for reaction (9), which compare reasonably well with the RRKM values derived in these studies: −165.7±12 kJ mol^{-1} for reaction (8) [35] and −147.8±12 kJ mol^{-1} for reaction (9).[50]

The germylene complexes possess rather large dipole moments (varying from 1.7 to 2.3 D) while the corresponding transition states are less polarized.[35,50] The calculated[35] charges in the reacting fragments of the complexes and transition states in the $GeH_2 + GeH_4$ system (absolute values in the range of 0.126–0.189 au in accordance with Mulliken population analysis, with GeH_2 bearing the negative charge) also indicate an increased polarity in the Ge—H insertion process. This polarity is even higher than for the $SiH_2 + SiH_4$ reaction (the absolute values of charges are in the range 0.069–0.112 au).[54]

The features of the PES of the systems under consideration obtained by quantum-chemical calculations favor our understanding of the experimental findings. The existence of a barrier to the second step of the process below the threshold energy of $EH_2 + E'H_4$ (E, E′ = Si, Ge) is sufficient to create a bottleneck on the Gibbs energy surface. This gives rise to a negative activation energy and variational behavior of the transition state. If such secondary barrier is too far below the threshold, its influence on the kinetics is minimal ($k_{-1} \ll k_2$, see Scheme 1). This is probably the case for the reaction of SiH_2 with SiH_4, where the calculated barrier lies 48 kJ mol^{-1} below the initial reactant energy and, according to the experimental data, the rates are virtually collision controlled.[54,55] The secondary barriers are much closer to the threshold energy for the reaction of GeH_2 with GeH_4 and especially for the reaction $GeH_2 + SiH_4$ (Table 5), which result in slower rates for the GeH_2 insertions compared to SiH_2 insertion. It seems likely that the second step, *viz.*, rearrangement of the pre-reaction complex (only **C1**), is fully rate-determining (*i.e.*, $k_{-1} \gg k_2$, see Scheme 1) for reaction (9). From these findings we may draw the inference that the second step is more difficult for germylenes inserting into E—H (E = Si, Ge) bonds than for silylenes.

GeH_2 + Et_3GeH. In contrast to the interaction of GeH_2 with EH_4 (E = Si, Ge), the reaction of GeH_2 with Et_3GeH was not affected by the total pressure in the range from 1 to 100 Torr.[51] This may be due to the more efficient redistribution of excess energy among the larger number of degrees of freedom of the product formed. The rate constants for insertion of GeH_2 (generated from DMGCP) into the Ge—H bond of Et_3GeH measured over a wide temperature range gave the Arrhenius parameters listed in Table 4. In general, this reaction is faster than reactions (8) and (9). Thus, alkyl substituents in the substrate enhance the insertion process. The activation energy for this reaction was found to be negative (even more negative than that for the $GeH_2 + EH_4$ reactions), which by analogy with the $GeH_2 + EH_4$ reactions can be best interpreted as proceeding *via* a weakly bound association complex (Scheme 2).

Scheme 2

$$Et_3Ge{-}H + GeH_2 \underset{k_{-1}}{\overset{k_1}{\rightleftharpoons}} Et_3Ge{-}H\cdots GeH_2 \xrightarrow{k_2} Et_3GeGeH_3$$

GeH_2 + $PhGeH_3$. A room-temperature kinetic study established that this reaction is at its high-pressure limit, if the total pressure in the system is above 10 Torr.[24] The temperature dependence of the rate constants was investigated in SF_6 using $PhGeH_3$ itself as the precursor of GeH_2 upon laser photolysis at 193 nm.[53] GeH_2 was monitored at 17111.31 cm^{-1}. In separate experiments it was shown that the room-temperature rate constant for the reaction of GeH_2 with benzene is nearly 300 times lower than that for the GeH_2 + $PhGeH_3$ reaction.[53] Thus, the latter reaction represents an insertion into Ge—H bonds rather than interaction with the aromatic ring. The Arrhenius parameters of this reaction are listed in Table 4. In contrast to the GeH_2 + Et_3GeH reaction, the activation energy of this reaction is similar to those of the reactions GeH_2 + GeH_4 and GeH_2 + SiH_4 (Table 4). Due to the high *A* factor, this reaction represents the fastest GeH_2 insertion process studied so far.

GeH_2 + Me_3SiH. The first absolute rate constant for the reaction of GeH_2 with Me_3SiH at room temperature was measured[23] using DMGCP as a photoprecursor and photolysis at 193 nm. This study gave a value of $(8.2\pm0.1)\cdot10^{-11}$ cm^3 $molecule^{-1}$ s^{-1} at 10 Torr total pressure independent of diluent, N_2 or SF_6. Later this measurement was repeated by Alexander *et al.*[24] using $PhGeH_3$ as a precursor. This gave rate constants of $(1.03\pm0.05)\cdot10^{-10}$ and $(0.92\pm0.11)\cdot10^{-10}$ cm^3 $molecule^{-1}$ s^{-1} at photolysis wavelengths of 193 and 248 nm, respectively. These values agree within experimental uncertainty with each other and are close to the previous value. They were found to be independent of pressure (up to 50 Torr) and bath gas (again N_2 or SF_6).

The temperature dependence of the rate constants for this insertion process has been studied in the temperature range 295–528 K using DMGCP as a precursor[52] and in the range 295–436 K using $PhGeH_3$ as precursor.[53] Laser photolysis of both precursors was carried out at 193 nm. Monitoring of GeH_2 was performed at 17111.31 cm^{-1}. Several checks of pressure dependence were performed at different temperatures, which confirmed that the reaction is not affected by the total pressure in the range 1–100 Torr.[52] GLC analysis of the final products of this reaction showed formation of the expected trimethylsilylgermane, Me_3SiGeH_3.[52] The Arrhenius parameters found by both groups are listed in Table 4. These values are very similar. The small discrepancies can be reasonably attributed to experimental uncertainty.

In the earlier studies on relative rates,[46] it was shown that the rate constant for the reaction of GeH_2 with Me_3SiH is two orders of magnitude lower than for the GeH_2 reactions with methylgermanes and Ge_2H_6 at 280 °C (553 K). This suggests that the rate constant for GeH_2 + Me_3SiH must be at least two orders of magnitude below the collision rate, *i.e.*, $<3\cdot10^{-12}$ cm^3 $molecule^{-1}$ s^{-1} at this temperature. However, the rate constant for this reaction found[52] at 528 K is $(1.03\pm0.05)\cdot10^{-11}$ and the rate constant calculated from the Arrhenius dependence (Table 4) for 555 K is $8.75\cdot10^{-12}$ cm^3 $molecule^{-1}$ s^{-1}. Thus, relative rate measurements[46] appear to underestimate the GeH_2 reactivity toward the Si—H bond of Me_3SiH.

Some general inferences from the studies of GeH_2 and $GeMe_2$ insertions into E—H bonds (E = Si, Ge). As can be seen from the data in Table 4, the presence of alkyl groups in the substrate (silane or germane) significantly enhances the insertion rate of GeH_2 into both Si—H and Ge—H bonds. The same effect but much less pronounced was demonstrated for the insertion reactions of different silylenes with methyl-substituted silanes.[10,56]

The results of the quantum-chemical calculations of the systems EH_2 + $E'H_4$ (E, E′ = Si, Ge) (see above) help to explain the dramatic effect of alkyl (Me, Et) groups in the substrates in terms of a loose collision association process (step 1, Scheme 1) with pre-reaction complex formation followed by a rearrangement *via* a tight transition state (step 2, Scheme 1).[10] If the barrier to the second step is close to rate determining, and its height is lowered by a substituent, then the rate will be significantly enhanced. Alkyl substituents in the substrate, due to their weak electron withdrawing effects (Pauling electronegativities of Si and Ge are smaller than those of C and H, with C being more electronegative than H) make the second, nucleophilic, step easier and the secondary barrier lower.[10] Because the barriers to the second step of GeH_2 insertion reactions were found[35,50] to be much closer to the overall reaction energy threshold compared to SiH_2 reactions,[54] the effect of alkyl substitution has to be more marked for the GeH_2 insertions. Smaller *A* factors for the GeH_2 reactions in comparison with those for the SiH_2 reactions (Table 4) also indicate that the GeH_2 reactions bottleneck is closer to the second step, especially for Si—H insertions. Thus, both the experimental and theoretical data suggest greater difficulty for the second step (Scheme 1) for GeH_2 compared to SiH_2.

The higher sensitivity of GeH_2 to substituents in the substrate means that this species is more selective than SiH_2. The increased selectivity of the GeH_2 species is illustrated by the data of Table 6 where the rate constants per E—H bond are compared in separate groups (I and II). The most striking feature is the high selectivity (a 25-fold difference per bond) shown by GeH_2 in the reactions with Me_3SiH and SiH_4. This is by a factor of 10-fold higher

Table 6. Comparison of gas-phase rate constants (k^{∞}/cm^3 molecule^{-1} s^{-1}) at room temperature (I) and elevated temperatures (II) (T/K) for insertion reactions of SiH_2 and GeH_2 into different Si—H and Ge—H bonds

Reaction	k^{∞} (T/K)		k_{rel}*		k'_{rel}*, **		Reference
	I	II	I	II	I	II	
$GeH_2 + GeH_4$	$5.5 \cdot 10^{-11}$ (292)	$2.0 \cdot 10^{-11}$ (520)	1	1	1	1	35
$GeH_2 + Et_3GeH$	$2.7 \cdot 10^{-10}$ (298)	$3.1 \cdot 10^{-11}$ (557)	4.9	1.6	19.6	6.2	51
$GeH_2 + Me_2GeH_2$	$2.4 \cdot 10^{-10}$ (297)	—	4.4		8.7		26
$GeH_2 + PhGeH_3$	$3.0 \cdot 10^{-10}$ (295)	—	5.5		7.3		24
$GeH_2 + SiH_4$	$1.3 \cdot 10^{-11}$ (295)	$5.3 \cdot 10^{-12}$ (554)	1	1	1	1	50
$GeH_2 + Me_3SiH$	$8.2 \cdot 10^{-11}$ (295)	$1.0 \cdot 10^{-11}$ (528)	6.3	1.9	25.2	7.6	52
$SiH_2 + SiH_4$	$4.6 \cdot 10^{-10}$ (296)	$2.6 \cdot 10^{-10}$ (578)	1	1	1	1	54
$SiH_2 + Me_3SiH$	$2.5 \cdot 10^{-10}$ (298)	$1.4 \cdot 10^{-10}$ (580)	0.5	0.5	2.2	2.2	10
$SiH_2 + Me_2SiH_2$	$3.3 \cdot 10^{-10}$ (298)	—	0.7		1.4		49
$GeH_2 + SiH_4$	$1.3 \cdot 10^{-11}$ (295)	$5.3 \cdot 10^{-12}$ (554)	1	1			50
$GeH_2 + GeH_4$	$5.5 \cdot 10^{-11}$ (292)	$2.0 \cdot 10^{-11}$ (520)	4.2	3.8			35
$GeH_2 + Me_3SiH$	$8.2 \cdot 10^{-11}$ (295)	$1.0 \cdot 10^{-11}$ (528)	1	1			52
$GeH_2 + Et_3GeH$	$2.7 \cdot 10^{-10}$ (298)	$3.1 \cdot 10^{-11}$ (557)	3.3	3.1			51
$SiH_2 + SiH_4$	$4.6 \cdot 10^{-10}$ (296)	$2.6 \cdot 10^{-10}$ (578)	1	1			54
$SiH_2 + GeH_4$	$3.1 \cdot 10^{-10}$ (295)	$2.0 \cdot 10^{-10}$ (553)	0.67	0.77			55

* The rate constant of the first reaction in each group is set to unity.
** k'_{rel} is the relative constant calculated per E—H bond.

than the corresponding selectivity of SiH_2. This selectivity can be compared with that of MeSiH (in the range 5-13 [59]) and $SiMe_2$ (*ca.* 90 [48]). Thus, for the Si—H insertion process, GeH_2 lies between MeSiH and $SiMe_2$, being the species of greatest discrimination in the series of EH_2 (E = C, Si, Ge).[52] It is also noteworthy that GeH_2 inserts more readily into Ge—H bonds than into Si—H bonds (Tables 4 and 6). This observation reflects the fact that Si—H bonds are stronger than Ge—H bonds,[60] although, in general, there is no linear correlation between the bond strength and insertion rates for heavy methylene analogs.[61] It is also worth noting that the phenyl group substitution in germane also remarkably enhances the GeH_2 insertion process,[53] probably decreasing the charge on the substrate Ge atom due to the mesomeric effect.

A comparison of collision efficiencies (ratios between the Lennard-Jones collision numbers and absolute rate constants) for different types of GeH_2 insertion and addition reactions showed that, at room temperature, the efficiencies are comparable for insertion into Si—H bonds and additions to alkenes and alkynes, while insertion into the Ge—H bond is characterized by higher efficiency.[53] A comparison of collision efficiencies for the reactions $SiH_2 + Me_3SiH$, $GeH_2 + Me_3SiH$ and $GeH_2 + Et_3GeH$ at different temperatures showed that all these reactions become collisionally controlled at low temperatures (just below room temperature) and there are no orientation requirements for any of these processes, or in other words the reactions have no steric factors.[52] This emphasizes the similarity between SiH_2 and GeH_2 insertion processes despite the fact that they are not quantitatively identical. The underlying reasons for their difference undoubtedly lies in the more diffuse nature of the germanium frontier orbitals with the increased divalent state stabilization energy (DSSE [62,63]) of GeH_2 compared to SiH_2.

As was shown in the beginning of this section, $GeMe_2$ is significantly less reactive than GeH_2. In silylenes, the rate decreasing effect of the methyl groups was attributed to the electron withdrawing ability of this group, which resulted in frontier orbital contraction, making the insertion process more difficult by increasing the barrier to the second step.[10,48] This should be valid for germylene as well. Yet another operating factor is the weakening of the pre-reaction complex.[26] Methyl groups are known to stabilize $SiMe_2$. It has a higher DSSE (128 kJ mol^{-1}) than SiH_2 (94 kJ mol^{-1}).[63] The more stable the silylene the weaker the bonding in the complex. This inference has been supported by several authors.[64—67] Destabilization of the complex means lowering the energy of its decomposition back into reactants relative to the energy of its transformation into final products and accounts for the switch to step 2 (Scheme 1) being fully rate determining and the high overall retardation of the insertion process. This consideration ought to be applicable to germylene reactions too.

$GeH_2 + H_2$. This is the simplest insertion reaction of all and has potentially great significance in germanium CVD systems where H_2 is present. While the kinetics of the silylene analog of this reaction has been well investigated,[10] the first kinetic and quantum-chemical study of

this GeH_2 reaction has been carried out only recently.[68] Following the logic of Jasinski[69] who investigated the reaction $SiH_2 + H_2$ by studying the $SiH_2 + D_2$ reaction, the kinetic investigation actually involved a study of the deuterium variant of the reaction (*viz.*, $GeH_2 + D_2$) in order to minimize potential complications arising from this third-body assisted association process at pressures below the high-pressure limit. The rate constant for the $GeH_2 + D_2$ reaction should approach the true rate constant for the bimolecular process because the initially-formed vibrationally excited GeH_2D_2 (GeH_2D_2*) can dissociate into GeHD + HD and $GeD_2 + H_2$ as well as $GeH_2 + D_2$. Thus, even if not stabilized, GeH_2D_2* undergoes a reverse dissociation into $GeH_2 + D_2$ to a minimum extent (unlike GeH_4*). The reaction was studied at 293 and 585 K at several partial pressures (up to 80 Torr) of D_2, but even at the maximum pressures the k_{obs} values were barely beyond the uncertainties of the measurements without D_2. Thus, no reaction was found and only upper limits for the second-order rate constant of $1.0 \cdot 10^{-14}$ at 293 K and $1.7 \cdot 10^{-14}$ cm^3 $molecule^{-1}$ s^{-1} at 585 K were obtained.[68] Both limiting values are close to each other; therefore, there was no point in checking intermediate temperatures. Thus, the magnitude of the true rate constant for this reaction remains to be determined.

On the basis of these limiting values, a lower limit for the activation energy for the reaction of GeH_2 with D_2 was estimated at 19.2±6 kJ mol^{-1}.[68] Thermochemical considerations of this process indicate that the true value of the activation energy should be in the range 63—84 kJ mol^{-1}. With the aim at deeper understanding of the difference between the fast reaction of SiH_2 with H_2 (reaction (12)) and reaction (13), quantum-chemical calculations of both systems were performed using high-level *ab initio* QCISD(T) and DFT B3LYP methods.[68]

$$SiH_2 + H_2 \longrightarrow SiH_4 \qquad (12)$$

$$GeH_2 + H_2 \longrightarrow GeH_4 \qquad (13)$$

From the theoretical point of view, reactions (12) and (13) are not only prototypes of silylene and germylene insertion into single bonds but also good test systems to check the accuracy of various quantum-chemical schemes used for studying the mechanisms of more complex reactions of heavy carbene analogs.

The PES of the SiH_2 insertion reaction (12) has previously been extensively studied at several different levels of theory. It was established that inclusion of electron correlation has a dramatic effect on both the shape of the PES and the barrier height.[70] The MP2/6-311G(d,p) calculations[70] revealed the presence of a weak pre-reaction complex on the PES of the $SiH_2 + H_2$ system. The calculations[68] at the QCISD(T)/6-311G++(3df,2pd)//QCISD/6-311G(d,p) and DFT B3LYP/6-311++G(3df,2pd) levels show that GeH_2 also forms a pre-reaction complex with H_2. The complexes and transition states of the SiH_2 and GeH_2 insertions are structurally similar. The results of the QCISD and B3LYP calculations are in good agreement with each other not only for the stable species (reactants and products) but also for the transition states (TS) and complexes. Selected geometric parameters of these structures calculated[68] by the QCISD/6-311G(d,p) method are shown in Fig. 3. The differences between the parameters of the silylene and germylene complexes are of the magnitude expected from the characteristic differences in the Ge—H and Si—H bond lengths.

The calculated energies are listed in Table 7. The pre-reaction complex in the germylene reaction is only about half as strong [ΔH(298K) = –9 (–11) kJ mol^{-1}] as that in the case of silylene [ΔH(298K) = –16 (–21) kJ mol^{-1}]. For these enthalpies the QCISD(T) values are given first, with the B3LYP values following in parentheses. Despite the weakness of these complexes the interactions of the two fragments are strong enough to stretch the H—H bond by 0.015 Å in the germylene complex and by 0.039 Å in the silylene complex.

The $\Delta H°$(13) values calculated by the QCISD and B3LYP methods are –168 and –157 kJ mol^{-1}, respectively (Table 7). Both of them fall in the range –147 to –168 kJ mol^{-1} estimated from experimental thermochemical data. The calculated barrier ($E_a = \Delta E$+ZPE) of 53 (50) kJ mol^{-1} at 298 K is slightly lower than the ther-

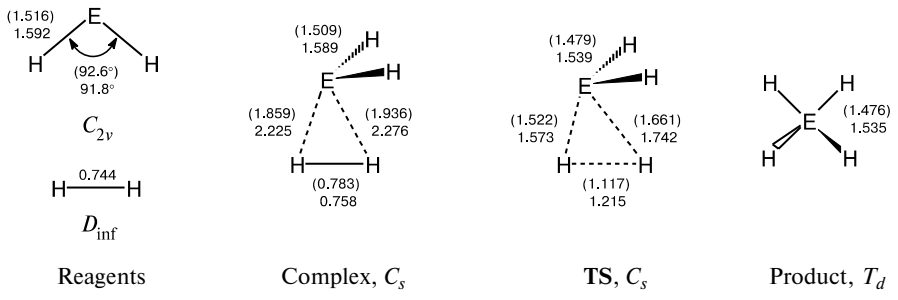

Fig. 3. Geometric parameters (R/Å) of structures corresponding to stationary points of the reactions of EH_2 (E = Si, Ge) with H_2, obtained from QCISD/6-311G(d,p) calculations. The values for E = Si are given in parentheses. The symmetry groups are given beside each structure label.

Table 7. QCISD(T)/6-311G++(3df,2pd)//QCISD/6-311G(d,p) and B3LYP/6-311++G(3df,2pd) calculated energies* (ΔE, ΔH, ΔG/kJ mol^{-1} at 298 K) of the stationary points on the PES of reactions $EH_2 + H_2 \rightarrow EH_4$ (E = Si, Ge)

State	ΔE + ZPE**	ΔE**	ΔH**	ΔG**
		SiH_2		
Complex	−9	−13	−16	15
	(−14)	(−19)	(−21)	(12)
Transition	13	7	5	38
state	(6)	(0)	(−2)	(33)
SiH_4	−226	−232	−234	−194
	(−225)	(−231)	(−234)	(−198)
		GeH_2		
Complex	−4	−6	−9	19
	(−5)	(−9)	(−11)	(20)
Transition	58	53	50	84
state	(56)	(50)	(48)	(83)
GeH_4	−160	−165	−168	−128
	(−150)	(−155)	(−157)	(−122)

* All energies are given relative to isolated $EH_2 + H_2$ species.
** QCISD(T) values and B3LYP values (in parentheses).

mochemical estimates (63—84 kJ mol^{-1} for 500 K). The reliability of the calculations may be judged by the results for the reaction (12) for which both methods give the same value of ΔH° equal to −234 kJ mol^{-1} (Table 7). This is in good agreement with the current best value[68] of −239±3 kJ mol^{-1}. The QCISD barrier, ΔE(12) of 7 kJ mol^{-1} is slightly higher than the measured E_a of −2 kJ mol^{-1}.[9] Even better agreement for the barrier ΔE(12) was obtained in B3LYP calculations (0 kJ mol^{-1}).

The calculations[68] show that, despite the mechanistic similarity, reaction (13) has a significant barrier compared to reaction (12), so a fast reaction of GeH_2 with H_2, like that of SiH_2 with H_2, is not to be expected. It prompts the question as to why there is a significant increase in the activation barrier from (12) to (13). The calculations[68] show unequivocally the extra extension of the H—H bond in the transition state of reaction (13) compared to reaction (12). This is consistent with the need to satisfy the less favorable H···Ge overlap compared to that of H...Si, due to the more diffuse nature of the germanium atomic orbitals. This reasoning also qualitatively supports a more demanding energy requirement for germylene than silylene in reaching the transition state.

1.4. Addition reactions

Additions to the multiple bonds of organic molecules represent another type of characteristic reactions of heavy carbene analogs.[2—5,9,10] These processes are suggested to start with formation of three-membered heterocyclic compounds: heterocyclopropanes and heterocyclopropenes in the case of addition to alkenes and alkynes, respectively. Further transformations of these compounds are believed to determine the set of final reaction products. The available kinetic data on the reactions of silylenes with alkenes and alkynes support this finding.[8—10] There are only a few cases where these cyclic compounds are stable enough to be isolated from the reaction mixtures.[3—5] The kinetic studies of germylene addition reactions will be considered here.

The first absolute gas-phase rate constants for addition reactions of GeH_2 [23,24] and $GeMe_2$ [25] (see Tables 1 and 2, respectively) were obtained at room temperature. A rough estimate of the room-temperature rate constant for the reaction of GeH_2 with benzene was $(1\pm1)\cdot10^{-12}$ cm^3 molecule^{-1} s^{-1}.[53] Some preliminary conclusions concerning mechanisms of the addition processes were made on the basis of these measurements.[23,25]

The observation of a strong pressure dependence for the reaction of $GeMe_2$ with ethylene and the lack of such a dependence when $GeMe_2$ reacts with *tert*-butylethylene (Table 2)[25] are consistent with the following mechanism:

Scheme 3

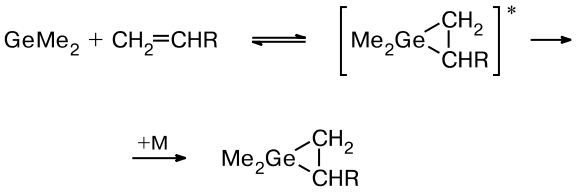

R = H, Bu^t

This mechanism corresponds to a three-body association process analogous to that found in the reactions of SiH_2 with alkenes.[10] It involves the initial formation of vibrationally excited germirane, which may then either redissociate or be collisionally stabilized. In the case of addition to C_2H_4, the germirane formed is sufficiently small to be relatively short lived with a high probability of redissociation. Preliminary RRKM modeling of this system suggested an energy release of *ca.* 55 kJ mol^{-1} in the ring formation.[25] As a result, this reaction shows a strong pressure dependence. The opposite situation occurs for the reaction of $GeMe_2$ with $Bu^tCH{=}CH_2$ where the germirane formed is bulky enough to be sufficiently long lived to have a high probability of collisional stabilization. This reaction showed a negligible pressure dependence over the same pressure range.

This mechanism is expected to operate for all GeH_2 reactions with alkenes. Although the pressure dependence of its addition to isobutene was not studied, the rate constant obtained is believed to be close to the high-pressure limiting value.[23]

GeH_2 reacts fast with buta-1,3-diene,[23] which apparently contradicts earlier studies[71] where no reaction prod-

uct could be found. However, the reason for this discrepancy may be the low stability of the expected germacyclopent-3-ene.[23] The detection of DMGCP among the photolysis products of $PhGeH_3$ in the presence of 2,3-dimethylbuta-1,3-diene in the gas phase,[23] supports high reactivity of GeH_2 with respect to 1,3-dienes. Similarly, $GeMe_2$ was successfully trapped by buta-1,3-diene upon laser photolysis of PMDG in the gas phase.[25] It was shown earlier[16,28] that the primary addition product of $GeMe_2$ to conjugated dienes is most probably a labile vinylgermirane formed upon 1,2-addition. This product then rearranges to the germacyclopentene,[5,28,29] the formal 1,4-adduct, or adds a second molecule of the diene to give 3,4-divinylgermacyclopent-3-ene.[4,16] Both reactions proceed simultaneously. Under the gas-phase conditions, the diene concentration is too low, thus rendering trapping of the initial 1,2-adduct highly unlikely. Thus, the following mechanism of the reactions of GeH_2 and $GeMe_2$ with dienes should operate in the gas phase (Scheme 4):

Scheme 4

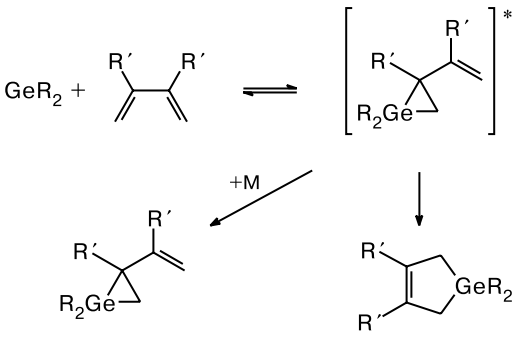

This mechanism is analogous to that of the reaction of silylenes with dienes.[10]

A comparison of the absolute rate constants for addition reactions of ER_2 (E = Si, Ge; R = H, Me) to alkenes, acetylene, and buta-1,3-diene at room temperature (Table 3) shows that introduction of methyl substituents in silylene and germylene decreases the rate constants by an order of magnitude. In general, GeH_2 and $GeMe_2$ are several times less reactive in the addition reactions than SiH_2 and $SiMe_2$, respectively.

In addition to room-temperature studies, the temperature dependences of rate constants for several prototype GeH_2 addition reactions have been studied. These results are considered below.

GeH_2 + ethylene. The kinetics of GeH_2 addition reactions to C_2H_4 [72] and C_2D_4 [73] were studied in the gas phase (with SF_6 as the bath gas) by the laser flash photolysis technique using DMGCP as a precursor, producing GeH_2 upon laser irradiation at 193 nm (Table 8). The consumption of GeH_2 was monitored at 17111.31 cm^{-1}. The pressure dependence of the rate constants for the $GeH_2 + C_2H_4$ reaction was successfully reproduced by RRKM modeling assuming germirane decomposition into ethylene and GeH_2 to be the reverse process with a critical energy (E_0 value) of 130 kJ mol^{-1}:

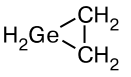

$$\longrightarrow \quad GeH_2 + CH_2{=}CH_2. \qquad (14)$$

Extrapolation of the observed rate constants with the aid of RRKM calculations gave the high-pressure limiting rate constants at each temperature, which follow the Arrhenius equation with the parameters listed in Table 8. The reaction of GeH_2 with ethylene slows down with an increase in temperature and the activation energy obtained for this reaction is negative (Table 8). The addition of GeH_2 to C_2D_4 was found to be pressure independent.[73] The rate constants for this reaction measured[73] at differ-

Table 8. Arrhenius parameters and high-pressure limiting rate constants for GeH_2 addition reactions and the corresponding reactions of SiH_2

Reaction	T/K	p/Torr	log$A$*	E_a /kJ mol^{-1}	$k^{\infty} \cdot 10^{10}$/cm^3 $molecule^{-1}$ s^{-1} (T/K)	Reference
$GeH_2 + C_2H_4$	293—555	1—100	−10.61±0.08	−5.4±0.6	2.1±0.4 (293)	72
$GeH_2 + C_2D_4$	295—554	1—100	−10.76±0.06	−5.8±0.5	1.76±0.06 (295)**	73
$GeH_2 + CH_2{=}CHMe$	293—415	1—100	−10.86±0.19	−7.2±1.2	2.7±0.6 (293)	74
$GeH_2 + C_2H_2$	295—436	1—50	−10.5±0.1	−3.5±0.3	1.38±0.04 (295)	53
	297—553	1—100	−10.94±0.05	−6.1±0.4	1.29±0.04 (297)	75
$SiH_2 + C_2H_4$	298—595	1—100	−9.97±0.03	−2.9±0.2	3.5±1.2 (298)	76
$SiH_2 + C_2D_4$	291—595	1—100	−9.97±0.03	−2.9±0.2	3.5±1.2 (291)	77
$SiH_2 + CH_2{=}CHMe$	294—520	1—100	−9.79±0.05	−1.9±0.3	3.4±0.2 (294)	78
$SiH_2 + C_2H_2$	291—613	1—100	−9.99±0.03	−3.3±0.2	3.5±0.6 (291)	79, 80

* A/cm^3 $molecule^{-1}$ s^{-1}.

** The reaction of GeH_2 with C_2D_4 is pressure independent; the rate constant listed was obtained directly from the kinetic measurements. As a result, its uncertainty is much smaller than the uncertainties of the other rate constants obtained by extrapolation of experimentally measured rate constants to infinite pressure.

ent temperatures coincided within experimental error with the high-pressure limiting rate constants obtained for the $GeH_2 + C_2H_4$ reaction.[72] Therefore, the Arrhenius parameters of both reactions also coincide (Table 8). For comparison the corresponding parameters of the reactions of SiH_2 with C_2H_4 [76] and C_2D_4 [77] are listed in Table 8.

The coincidence of the Arrhenius parameters for the reactions of GeH_2 with ethylene and ethylene-d_4 suggests that secondary isotope effects for this reaction are close to unity.[73] The absence (within the limits of experimental error) of a secondary deuterium effect was earlier demonstrated for SiH_2 addition reactions with C_2H_2/C_2D_2,[79,80] and C_2H_4/C_2D_4 [76,77]and for the SiH_2 and SiD_2 additions to CH_3CHO.[81,82] Theoretical values of this effect (k_H/k_D) for the latter pair of reactions were predicted to lie in the range 1.10–1.25.[82] This suggests a value close to unity for the secondary isotopic effects in all the addition reactions of SiH_2 and GeH_2 mentioned above, which is in agreement with experimental data. The coincidence of the measured rate constants for $GeH_2 + C_2D_4$ with those obtained by extrapolation to infinite pressure for $GeH_2 + C_2H_4$ supports the correctness of the extrapolation. It is noteworthy that the comparative study of the kinetics of the reactions of GeH_2 with C_2H_4 and C_2D_4 is the first example of an investigation of the kinetic isotope effects in germylene chemistry.

The pressure dependence of the second-order rate constants for $GeH_2 + C_2H_4$ implies reversibility in the initial addition stage.[72] The lack of the pressure dependence for the reaction $GeH_2 + C_2D_4$ suggests that the reaction does not represent a simple third-body assisted association reaction, as suggested above, but its mechanism also involves an isotope scrambling process, leading to H/D exchange within the initially formed vibrationally-excited species before its dissociation to reactants.[73] The involvement of such isotope scrambling processes has already been shown for the SiH_2 addition reactions with ethylene[77] and acetylene.[80] As a result, in addition to dissociation into $GeH_2 + C_2D_4$ alone, this vibrationally-excited species may also give pairs $GeHD + C_2D_3H$ and $GeD_2 + C_2D_2H_2$. Thus, removal of GeH_2 from the reaction system will be less dependent on the efficiency of stabilization of the initially formed vibrationally excited species by collisions with a third molecule, *i.e.*, on the total pressure in the system. If this scrambling process is effective enough, the rate constants measured by monitoring GeH_2 only will be only slightly pressure dependent or completely pressure independent. By analogy with the reactions of SiH_2 with ethylene[77] and acetylene[80] a plausible scrambling process is the following (Scheme 5).[73]

In accordance with this scheme, the statistical probability of dissociation to GeH_2 is 6.7%. This is derived by considering the probability as the ratio of the number of

Scheme 5

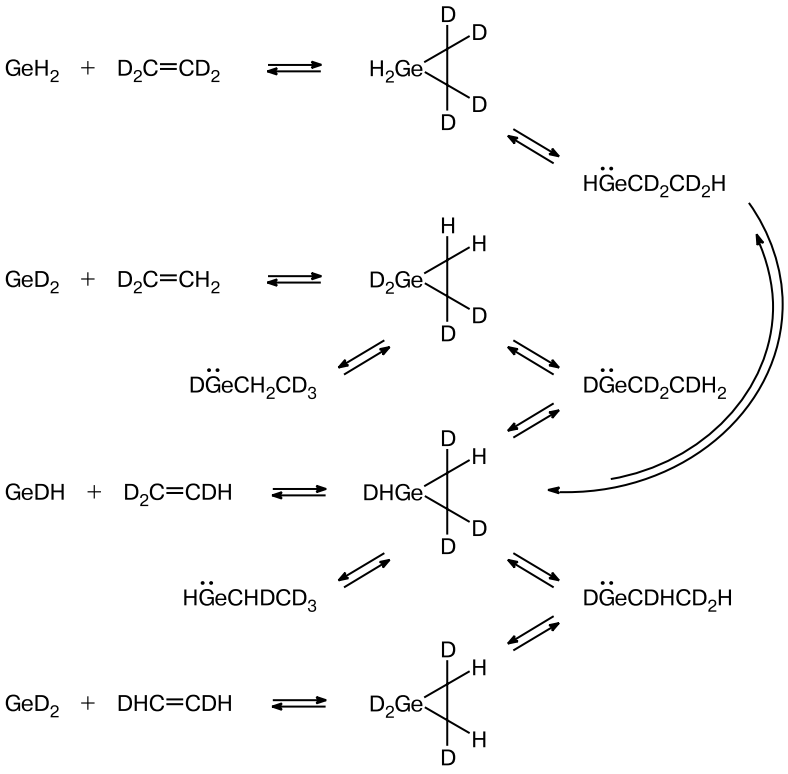

pathways leading back to GeH_2 to all possible decomposition pathways of all possible germirane-d_4 isomers, which is equal to 1/15. Thus, provided it is fast, this isotopic scrambling process enables virtually irreversible removal of GeH_2, and the measured rate constants for $GeH_2 + C_2D_4$ should correspond to the true bimolecular addition reaction. A quantum-chemical study of the PES of the $GeH_2 + C_2H_4$ system confirms that this process is energetically possible.[72] Several fragments of the PES of the GeC_2H_6 system were studied[83] by the MP2 and QCISD methods. Five singlet and four triplet structures were found.[83] The singlet structures comprised germirane, vinylgermane, 1-germapropene, ethylgermylene, and the transition state of internal rotation around the C—Ge bond in ethylgermylene. Based on the QCISD calculated energies, vinylgermane was found to be the most stable among these singlet species.[83] The energies of the triplet states of all these species were found to be at least 103 kJ mol^{-1} higher than those of the corresponding singlet structures. The transition states of the addition reaction $GeH_2 + C_2H_4$ and subsequent conversions of germirane were not considered.[83]

Ab initio (G2//MP2/6-31G(d) and G2//QCISD/6-31G(d)) and DFT (B3LYP/6-31G(d)) quantum-chemical calculations of the PES of the $GeH_2 + C_2H_4$ system revealed seven minima which lie below the energy of the reactants and eight transition states connecting these minima (Fig. 4).[72] Except for vinylgermane, all the minima correspond to highly reactive derivatives of germanium, *viz.*, germylenes, germaethenes (germenes), germirane, and a π-complex. The B3LYP and QCISD calculated geometric parameters agree well with each other for the species where both have been carried out. B3LYP and G2 calculations predict the same order of stability for all minima except for the π-complex and 1-germapropene (Fig. 4). It seems that the B3LYP method underestimates the stability of the system $GeH_2 + C_2H_4$, because the relative energies obtained at the B3LYP level are always lower than those found at the G2 level. Surprisingly, the most stable isomer on the PES is dimethylgermylene, a highly reactive divalent germanium species.[72] A comparison of the relative energies for the limited set of the GeC_2H_6 isomers calculated by the QCISD(T)/6-311G(3df,2p) method[83] and those obtained from more extensive G2 calculations[72] shows that for the same structures the differences are less than 3 kJ mol^{-1} (the energies were compared with those of vinylgermane).

According to both the B3LYP and QCISD calculations, the reaction of GeH_2 with C_2H_4 results initially in the formation of the π-complex corresponding to a rather shallow minimum on the PES. The barrier (**TS3**, Fig. 4) separating the complex from germirane is only 9 kJ mol^{-1}

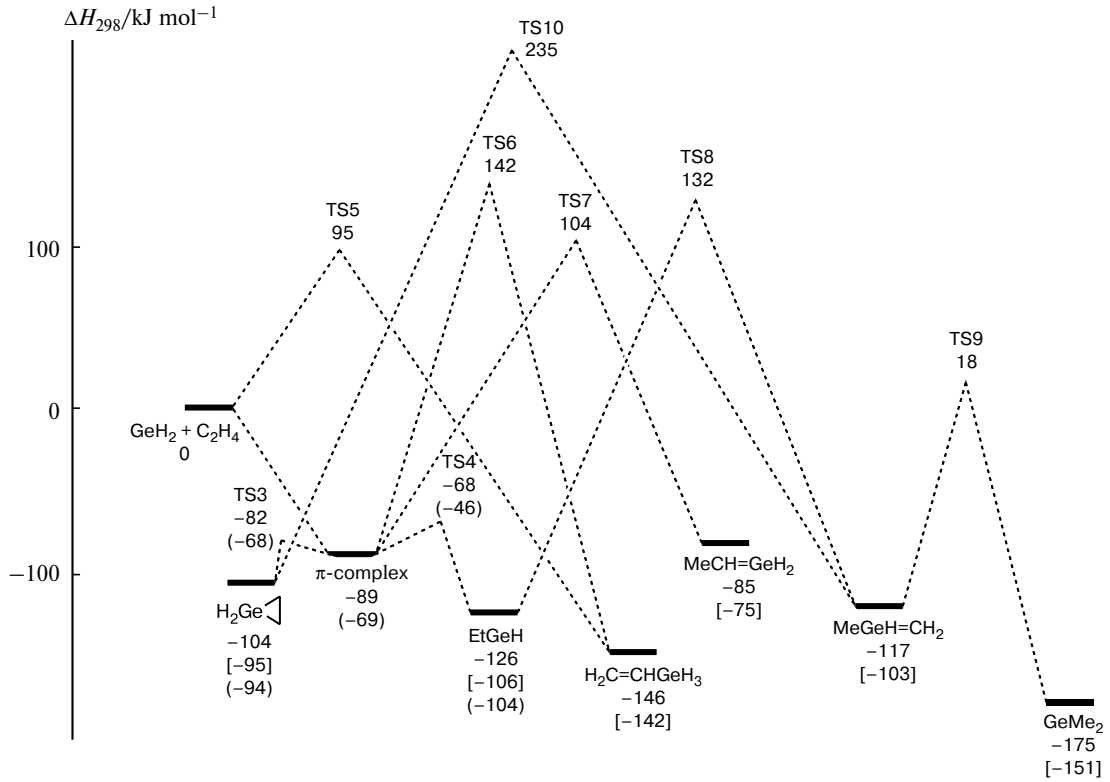

Fig. 4. Potential energy (enthalpy at 298 K) surface of the reaction $GeH_2 + C_2H_4$, obtained from calculations: B3LYP/6-31G(d), G2 (figures in brackets), and G2//QCISD (figures in parentheses).

(B3LYP) or 3 kJ mol^{-1} (G2//QCISD) at 0 K. The extremely low barrier **TS3** means that in practice the π-complex collapses to germirane almost without hindrance. On the other hand, apart from the extremely high-energy pathway through **TS10**, the only pathway from germirane to other products is *via* the π-complex. This implies that as far as further steps are concerned the π-complex and germirane are essentially indistinguishable.

All attempts to locate the π-complex by the MP2 method using basis sets ranging from 6-31G(d) to 6-311G(d,p) failed. The reaction path connecting $GeH_2 + C_2H_4$ to germirane represents a continuous downhill process albeit with a small plateau at Ge—C distances typical of the complex.[72] However, this complex was found in previous quantum-chemical studies using MP2 valence-only calculations in conjunction with an effective core potential[84] and also in B3LYP/6-31G* calculations.[85] Because the QCISD method provides a better treatment of electron correlation than MP2, its prediction of the existence of the π-complex seems reliable, and is in agreement with the results of DFT calculations.

The energies of germirane and the π-complex obtained in quantum-chemical calculations at different levels[72,84—86] are in reasonable agreement. In particular, the ΔH° values for germirane decomposition equal to 126 [86] and 103 [84] kJ mol^{-1} were obtained on the basis of *ab initio* calculations and thermochemical reasoning, although using *ab initio* means alone (MP4/6-31G(d,p)) gave too low a value of ΔE^0 + ZPE (at 0 K) of 51.9 kJ mol^{-1}.[84] DFT calculations (B3LYP/6-31G*) of germirane decomposition[85] resulted in the value of 115 kJ mol^{-1} for ΔH°.

Besides the π-complex and germirane, the only other accessible product of the reaction of GeH_2 with C_2H_4 is ethylgermylene (Fig. 4), a highly reactive species. Because the previous calculations[84—86] restricted the search for the GeC_2H_6 potential energy surface to formation of germirane from $GeH_2 + C_2H_4$, this pathway has not been found. Ethylgermylene is separated from the π-complex by a low-energy barrier (**TS4**) and is more thermodynamically stable than germirane (Fig. 4). Its formation from both the π-complex and germirane (*via* the π-complex) presents no problem since **TS4** lies well below the reaction energy threshold. It is worth noting that the overall barrier to germirane rearrangement into ethylgermylene *via* **TS3**, the π-complex, and **TS4** is only 36 kJ mol^{-1} (B3LYP value), which explains the known difficulties of its preparation and suggests that replacement of the H atoms at Ge by other substituents may slow down the rearrangement process. Indeed, several germiranes stable in an inert atmosphere have been reported to date,[87,88] but none of them contains an H atom at Ge. Formation of other potential products of the reaction $GeH_2 + C_2H_4$ would require the overcoming of high energy barriers (**TS5**—**TS10**). It is therefore unlikely that these products would be formed under the experimental conditions of the kinetic study.

Besides the reaction pathways on the closed-shell PES of the system $GeH_2 + C_2H_4$, one can suggest another pathway *via* a biradical structure like $\dot{G}eH_2CH_2\dot{C}H_2$.

$$GeH_2 + H_2C{=}CH_2 \longrightarrow \dot{G}eH_2CH_2\dot{C}H_2. \qquad (15)$$

However, thermochemical estimation showed[72] that formation of such biradical is an endothermic process with an energy of 40—70 kJ mol^{-1} and therefore this pathway should not operate in this kinetic experiment. This is the reason why the biradical pathway was not investigated in the quantum-chemical calculations.[72]

One of the outputs of the quantum-chemical study is that the assumption of the RRKM modeling about correspondence of the pressure dependence of the $GeH_2 + C_2H_4$ reaction to unimolecular decomposition of germirane is not correct.[72] The observation of the pressure dependence in this system must be ascribed to a third-body association process with two products, *viz.*, germirane and ethylgermylene. The initially formed vibrationally-excited species, *viz.*, the π-complex, can redissociate or be stabilized to give either germirane or ethylgermylene depending on the relative propensities to cross **TS3** or **TS4** at the excitation energy involved. However, it has been argued[72] that the RRKM modeling of the $GeH_2 + C_2H_4$ reaction can be considered as a reasonable approximation to the real process. This is because the *A* factor employed corresponds to the formation of the π-complex, while the E_0 value corresponds to the energy of the lowest accessible product, *i.e.*, ethylgermylene rather than germirane.

This reflects a further important finding of this study, *viz.*, that germirane easily and reversibly rearranges to ethylgermylene,[72] which is in complete agreement with the suggested scheme of a scrambling process (see above).[73]

It is interesting to compare the PES of the $SiH_2 + C_2H_4$ and $GeH_2 + C_2H_4$ systems. Figure 5 shows fragments of the PES of these systems according to calculations.[72,89] In contrast to the exothermic nature of the rearrangement of germirane to ethylgermylene,[72] an analogous silirane rearrangement is endothermic, although the transition state of the latter reaction lies below the energy of $SiH_2 + C_2H_4$.[89] This explains why the reaction $GeH_2 + C_2D_4$ does not show any pressure dependence, while for $SiH_2 + C_2D_4$ a small effect is observed.[77] Because of the endothermicity of the isomerization of silirane to ethylsilylene, the efficiency of the scrambling process is lesser in this case than in the case of the exothermic rearrangement of germirane to ethylgermylene. As has been discussed above, the occurrence of this isomerization of silirane to ethylsilylene was experimentally demonstrated by observed isotope exchange during the reaction of SiH_2 with C_2D_4.[77]

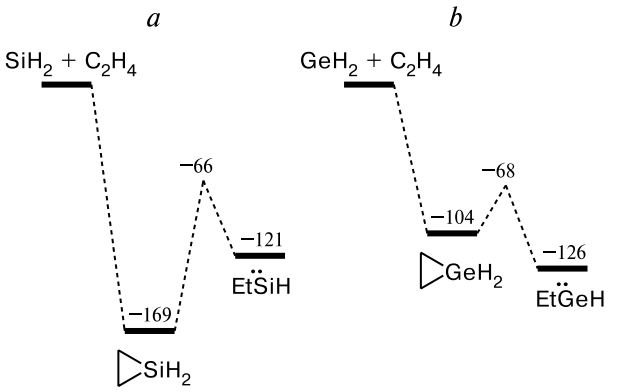

Fig. 5. Comparison of the energies of selected species on the PES of the $SiH_2 + C_2H_4$ and $GeH_2 + C_2H_4$ systems: (12/12)CASPT2N/6-31G* calculations[86] (*a*) and B3LYP/6-31G(d) calculations[72] (*b*) (π-complex is not shown). The relative energies are given in kJ mol^{-1}.

A similar order of the relative stabilities of the three-membered heterocycles and isomeric heavy carbene analogs was revealed for systems EC_3H_8 (E = Si, Ge). Calculations at the MP2/6-311G**//MP2/6-31G* level revealed that ethylmethylgermylene is more stable than 1-methylgermirane, but ethylmethylsilylene is less stable than 1-methylsilirane.[90,91] Thus, the main difference between the additions of GeH_2 and SiH_2 to ethylene consists in the end product of the reactions. While the SiH_2 addition leads to the formation of silacyclopropane, the major end product of GeH_2 addition is rather ethylgermylene.

The system GeH_2 + propene. A time-resolved study of this reaction was carried out in the gas phase in the temperature range 293–415 K and at total pressures (with SF_6 as the bath gas) varying from 1 to 100 Torr.[74] GeH_2 was generated by laser flash photolysis of DMGCP at 193 nm and monitored at 17111.31 cm^{-1}. Further increase in temperature up to 476 K resulted in scatter and irreproducibility of the rate measurements suggesting the involvement of side processes in the system at such elevated temperatures. The reaction showed a strong pressure dependence characteristic of a third-body mediated association reaction. Extrapolation of the measured rate constants to infinite pressure using the RRKM theory applied to the following reverse reaction:

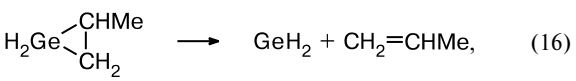

gave the high-pressure limiting rate constants, k^{∞}.

The Arrhenius parameters calculated from the temperature dependence of k^{∞} are presented in Table 8. Although this reaction is expected to form propylgermylene in addition to methylgermirane, by analogy with the reaction $GeH_2 + C_2H_4$,[72,73] the correctness of the RRKM-assisted extrapolation of the rate constants has already been demonstrated.[72,73] The reaction of GeH_2 with propene was found to slow down with an increase in temperature just like the reaction $GeH_2 + C_2H_4$.

Theoretical calculations of the germylene[72,84–86] and silylene[78,89,92] addition reactions indicate that these processes involve two distinct stages, an initial π-attack or the "electrophilic stage" (transfer of alkene π-electrons to the empty p-orbital of the carbene analog) followed by σ-attack or the "nucleophilic stage" (transfer of the carbene-analog lone pair electrons to the π*-orbital of alkene), although the formation of an intermediate pre-reaction π-complex is characteristic of germylene reactions only. Methyl substituents in the alkene are believed to enhance the rates of electrophilic processes by facilitating the transfer of C=C π-electrons. However, the rates of GeH_2 additions to C_3H_6 and C_2H_4 are virtually identical (Table 8), being at room temperature very close to the rate constant for GeH_2 addition to isobutene.[23] Thus, methyl substituents in the alkene have almost no effect. It is hardly surprising, since the reaction rates are very close to their collision limits (collision efficiencies are 48% and 59% for the GeH_2 additions to C_2H_4 and C_3H_6, respectively[74]). The same is true for the corresponding SiH_2 additions.[76,78]

The system GeH_2 + acetylene. The room-temperature rate constant for this reaction in the gas phase was measured using both DMGCP [23] and $PhGeH_3$ [24] as precursors (Table 1). It was shown to be pressure independent within the pressure range 10–50 Torr.[24] In more extensive investigations (using $PhGeH_3$ as precursor) second-order rate constants were obtained in the temperature range 295–436 K at a total pressure of 10 Torr.[53] The Arrhenius parameters determined from these rate constants turned out to be very close to those of the reaction $SiH_2 + C_2H_2$ (Table 8), which suggested the quantitative resemblance of the mechanisms of both reactions.[53] Possible pressure dependence of the rate constants at elevated temperatures was not checked, because it was assumed that the reaction also approached the high-pressure limit at these temperatures, despite the fact that similar addition reactions of GeH_2 to C_2H_4 [72] and of SiH_2 to both C_2H_4 [76] and C_2H_2 [79] showed a pressure dependence in the pressure range 1–100 Torr. Later, this reaction was reinvestigated in the wider temperature range (297–553 K) and in the pressure range 1–100 Torr using DMGCP as a precursor[75] and it was found that the reaction does show a slight pressure dependence at higher temperatures. Based on the high-pressure limiting rate constants (obtained by eyeball extrapolation), the Arrhenius parameters were determined[75] which were slightly different from those already reported[53] (Table 8). These differences can be put down to uncertainties in the experimental rate constants.

An attempt at RRKM modeling of the observed pressure dependence based on the following reaction scheme

(which actually is analogous to the scheme used in the RRKM modeling of the $GeH_2 + C_2H_4$ system, see above), failed:

$$H\ddot{G}eCH{=}CH_2 \rightleftharpoons H_2Ge\triangleleft \longrightarrow \longrightarrow GeH_2 + C_2H_2 \quad (17)$$

An unreasonably high value of the critical energy (305 kJ mol^{-1}) was found to be necessary to reproduce the experimental pressure dependence.[75] This implied the existence of an additional, irreversible, reaction channel, efficiently removing the vibrationally excited intermediate prior to stabilization. Therefore, a more complicated scheme, which includes such an irreversible reaction channel leading to ethylene and atomic Ge, was considered (Scheme 6).

Scheme 6

$$H\ddot{G}eCH{=}CH_2 \xleftarrow{+M} H\ddot{G}eCH{=}CH_2^* \quad (a \rightleftharpoons,\ b \searrow)$$

$$GeH_2 + C_2H_2 \qquad Ge(^3P_1) + H_2C{=}CH_2$$

It is noteworthy that GC-analysis of the products revealed formation of ethylene as the only product detectable in significant amounts.[75] Using the RRKM theory, it was shown that this more extended Scheme 6 would satisfy the observed slight dependence of the reaction rate on pressure if the critical energy of the new decomposition pathway *b* (in Scheme 6) of vinylgermylene was *ca.* 146 kJ mol^{-1}.

Further information concerning the reaction $GeH_2 + C_2H_2$ was obtained from a quantum-chemical study of the PES of this system. It was done by DFT (B3LYP/6-31G(d)) and *ab initio* (G2//MP2(full)/6-31G(d), G2(MP2,SVP)//B3LYP/6-31G(d), and G2(MP2,SVP)//QCISD/6-31G(d)) methods.[75] The structures corresponding to the stationary points located on the PES are shown in Fig. 6. Except for ethynylgermane, all the minima correspond to highly reactive derivatives of germanium. This situation is similar to that observed for the $GeH_2 + C_2H_4$ system (see above). The large number of species and transition states indicate that there is considerable complexity in the mechanism of the reaction $GeH_2 + C_2H_2$. The geometric parameters obtained for the local minima and transition states at different levels of theory agree well with one another. Table 9 collects the enthalpy values for the minima and transition states. In general, a similar order of stability for most of the structures was obtained in both B3LYP and G2 calculations, although for several species close in energy their particular ordering was changed on going from one computational method to another. Again, the B3LYP method seems to underestimate the stability of the reactants GeH_2

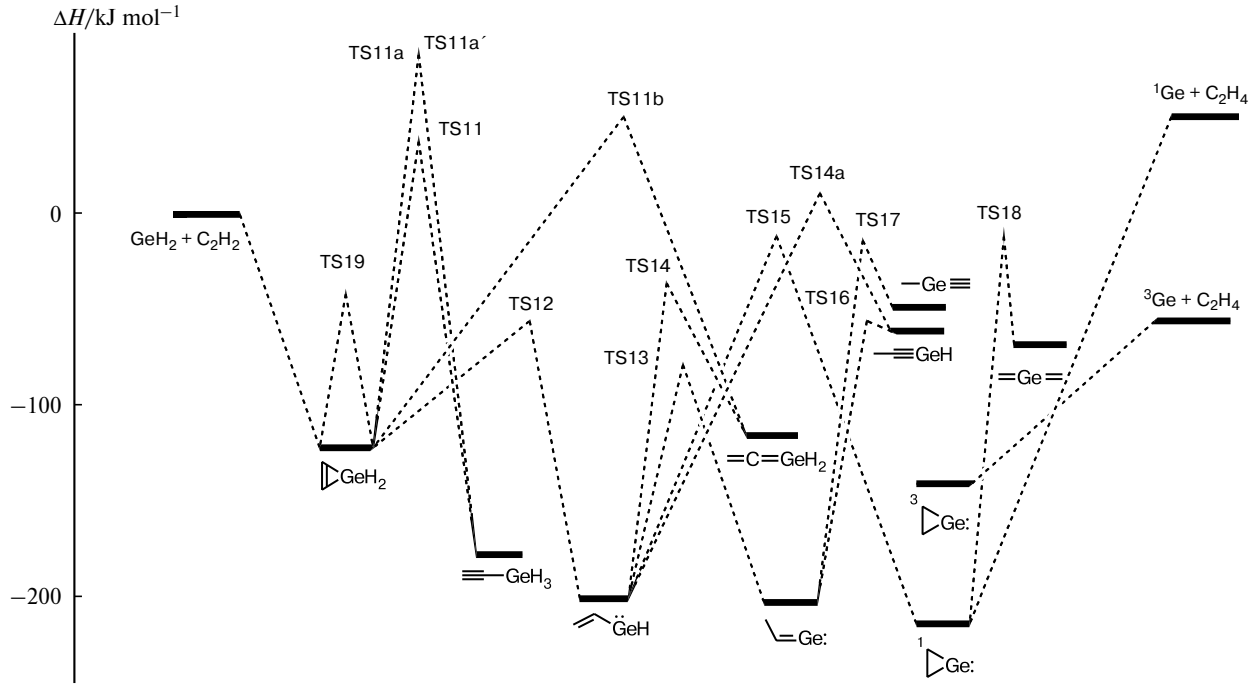

Fig. 6. Potential energy (enthalpy) surface of reaction $GeH_2 + C_2H_2$. The enthalpy values (see Table 9) were obtained from density functional B3LYP/6-31G(d) calculations.

Table 9. B3LYP/6-31G(d) (I), G2(MP2,SVP)//B3LYP/6-31G(d) (II), and G2(MP2,SVP)//QCISD/6-31G(d) (III) calculated relative enthalpies (ΔH at 298 K) of the stationary points on the PES of the GeC_2H_4 system

Stationary points	ΔH/kJ mol^{-1}		
	I	II	III
$GeH_2 + C_2H_2$	0	0	0
Germirene, 	−132	−108	−107
Ethynylgermane, 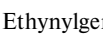	−187	−169	−170
Vinylgermylene , 	−207	−168	−166
1-germaallene, 	−124	−89	−89
1-germapropenylidene, 	−210	−175	−172
2-germapropyne, 	−55	−31	−31
1-germapropyne, 	−66	−29	−33
1-germiranylidene (S), 	−222	−187	−183
2-germaallene,	−73	−44	−43
1-germiranylidene (T), 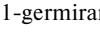	−152	−94	—
$^1Ge + C_2H_4$	50	35	37
$^3Ge + C_2H_4$	−61	−39	−37
TS11	35	46	47
TS11a	63	82	81
TS11a´	62	84	84
TS11b	47	89	89
TS12	−56	−28	−26
TS13	−86	−51	−49
TS14	−58	−7	−6
TS14a	12	61	63
TS15	−20	6	8
TS16	−69	−25	−23
TS17	−19	15	17
TS18	−16	13	14
TS19	−48	−29	−29

and C_2H_2, because the energies obtained at the B3LYP level are always lower than those found at the G2 level. The most stable isomer on the PES is 1-germiranylidene, a highly reactive divalent germanium species containing a strained three-membered ring.

According to the calculations, the initial reaction of GeH_2 with C_2H_2 results in the formation of germirene. In contrast to the reaction $GeH_2 + C_2H_4$, the formation of a pre-reaction π-complex was not found for the system $GeH_2 + C_2H_2$, although the transition state **TS19**, which corresponds to the degenerate process of rotation of the GeH_2 group within germirene, can be considered as the missing π-complex. Germirene readily rearranges to vinylgermylene. This isomerization route is particularly facile, having a barrier of only 76 kJ mol^{-1} (B3LYP). Thus, the germirene rings in general are expected to be unstable if they contain an H atom at Ge. The only germirenes isolated so far have two substituents at the Ge atom.[87,93,94] Vinylgermylene may then easily give 1-germapropenylidene *via* **TS13** or 1-germaallene *via* **TS14**. 1-Germaallene lies much higher in energy than 1-germapropenylidene and will rearrange back to the latter. Thus, this species is insignificant for the overall mechanism.

The formation of 1-germapropenylidene is quite probable. At the same time, it is a mechanistic dead end, because there is no low-energy pathway leading from this species to a more stable one.

A more attractive pathway from vinylgermylene seems to be that resulting in the formation of 1-germiranylidene involving **TS15**. It was shown at the B3LYP level, that, once formed, 1-germiranylidene may dissociate into $Ge(^3P_1)$ and ethylene due to intersystem crossing to the triplet surface, thus representing the irreversible reaction channel suggested by the RRKM modeling. It is also worth noting that a similar pathway linking 1-germapropenylidene to $Ge(^3P_1)$ and C_2H_4 was not found.

Because surmounting the lower **TS13** barrier leads to a mechanistic dead end and therefore 1-germapropenylidene will rearrange back to vinylgermylene, if not stabilized by collisions, the pathway through the higher barrier **TS15** might successfully compete with the pathway through **TS13**. Despite the fact that **TS15** was found to lie somewhat above the overall reaction threshold by 6 or 8 kJ mol^{-1} (according to G2 calculations), although below the threshold by 20 kJ mol^{-1} (in the B3LYP calculations), the pathway through this transition state represents the only pathway found so far that might explain the experimental observations. However, according to the quantum-chemical calculations (Table 9), **TS15** is higher in energy by 187 (B3LYP) or 174 (G2) kJ mol^{-1} than vinygermylene. These values are considerably larger than 146 kJ mol^{-1} found for the required critical energy in the RRKM estimations discussed above. Thus, in spite of the complexity of the GeC_2H_4 potential energy surface revealed by the quantum-chemical calculations, the pathways found cannot at present be fully reconciled with the kinetic observation of the lack of a pressure dependence in the $GeH_2 + C_2H_2$ reaction system. It should also be noted that thermochemical estimates[75] suggest that involvement in the reaction mechanism of biradical species might also reproduce the energetics obtained from experiment. However, extensive quantum-chemical calculations aimed at finding such biradical species failed.

A number of the PES fragments for the GeC_2H_4 system were previously explored[83] with the MP2 method. Singlet and triplet structures of 1-germiranylidene and a π-complex of GeH_2 with C_2H_2 were found. Strangely enough, the calculations[83] did not reveal the germirene structure found in the B3LYP and QCISD calculations,[75] but located the structure of a weakly bonded π-complex, which, according to the B3LYP and QCISD calculations, is not a local minimum.[75] This is particularly un-

usual, because the previous study of the PES of the GeH_2 + ethylene system showed[72] that both methods (B3LYP and QCISD) correctly describe the formation of the π-complex between GeH_2 and ethylene, contrary to the results of the MP2 calculations,[72] which show that the π-complex is unstable and rearranges into germirane without an activation barrier.

There are several theoretical investigations of the SiC_2H_4 potential energy surface,[95–97] although none involved the whole range of molecular and transition state analogous to those found on the PES of the GeC_2H_4 system.[75] Both experimental[80] and theoretical[95,96] data support the isomerization of the initially formed silirene into vinylsilylene through a low-energy transition state. But this isomerization is slightly endothermic in contrast to analogous germirene rearrangement.[75] Thus, this reversal of the relative stabilities of the three-membered heterocycles and their heavy carbene isomers on going from Si to Ge, parallels that of the SiC_2H_6 and GeC_2H_6 potential energy surfaces.[72,89] Another contrast between the reactions of SiH_2 and GeH_2 with C_2H_2 is that, in the former, there is an energetically accessible route to ethynylsilane, while the corresponding pathway to ethynylgermane requires passage through a transition state lying above the threshold (see Fig. 6).

General remarks on the addition processes. Like the insertion processes, GeH_2 addition reactions are characterized by lower A factors and slightly more negative E_a values than their SiH_2 counterparts (Table 8). Nevertheless, all the GeH_2 addition reactions studied are fast. Their rate constants at room temperature correspond to 30–60% of the Lennard-Jones collision numbers.[74] The collision efficiencies of the corresponding SiH_2 reactions are 60–80%.[74] In other words, the efficiencies of the GeH_2 reactions are almost as high as those of the SiH_2 reactions, but because of larger negative E_a values the GeH_2 reaction rates will approach those of SiH_2 only at sub-ambient temperatures becoming encounter controlled.

The negative activation energies found for GeH_2 addition reactions suggest the involvement of intermediate complexes. Indeed, a pre-reaction complex was found in quantum-chemical calculations of the reaction of GeH_2 with C_2H_4 [72,84,85] (but not found in calculations of the reaction of GeH_2 with C_2H_2 [75]). However, to play a kinetic role, such complexes must have the capability to redissociate into reactants (under high-pressure conditions). The π-complex found by calculation does not fulfill this requirement as it lies too low in energy compared to the reactants and furthermore no other species suitable for playing such a role was found either. We must therefore conclude that the negative activation energies of the GeH_2 addition reactions with alkenes and acetylene discussed above arise from angular momentum effects in a normal third-body assisted association.[98,99]

1.5. Reactions with O-donor molecules

Gas-phase rate measurements have been carried out for reactions of GeH_2 with D_2O, Me_2O, MeOH, and CD_3OD at room temperature (295 K) in the pressure range 10–200 Torr (with SF_6 as the bath gas), using $PhGeH_3$ as a precursor.[100] The rate constants obtained are collected in Table 10.

The reaction of GeH_2 with D_2O was found to be very slow.[100] As a result, the rate constants were determined with large uncertainties (Table 10). A similar reaction of SiH_2 with H_2O is also slow.[65,101,102] Quantum-chemical calculations[66,103] showed that the reaction $GeH_2 + H_2O$ involves the formation of a pre-reaction complex. Therefore, the deuterium effect is a secondary isotope effect, which typically results in a small decrease in the high-pressure limiting rate constants. However, at the low pressures in the fall-off region, deuterated reactants usually show larger rate constants (an inverse isotope effect) than their hydrogenated counterparts.[98] In the kinetic studies of SiH_2 reactions with O-donor molecules, it was inferred that the high-pressure limit for such reactions is reached at pressures $>10^5$ Torr.[65,101,102] The reaction of GeH_2 with H_2O was expected to have a similar pressure dependence, and the pressure range used was far from the high-pressure limit. Partly because of this, the rates were very slow and near the limit of experimental measurement. In fact, the values obtained for the rate constants measured for the reaction $GeH_2 + D_2O$ at 30 and 100 Torr (with SF_6 as the bath gas) were nominally the same.[100] Because the reaction $GeH_2 + D_2O$ was expected to be faster than the reaction $GeH_2 + H_2O$, the kinetics of the latter were not studied.[100]

The reactions of GeH_2 with Me_2O, MeOH, and CD_3OD are much faster and show clear pressure dependences (see Table 10). All of them remain in the fall-off region up to pressures of 200 Torr at least.[100] Deuterated

Table 10. Room-temperature rate constants (k^∞) for reactions of GeH_2 with D_2O, Me_2O, MeOH, and CD_3OD at different total pressures[100]

p/Torr	$k^\infty \cdot 10^{11}$/cm^3 molecule^{-1} s^{-1}			
	D_2O	Me_2O	MeOH	CD_3OD
10	—	0.79±0.03	0.11±0.03	0.41±0.01
30	$(8\pm4)\cdot10^{-2}$	2.15±0.07	—	—
50	—	2.83±0.12	0.80±0.04	1.14±0.03
70	—	—	—	1.66±0.03
80	—	—	—	1.45±0.01
100	$(8\pm6)\cdot10^{-2}$	4.85±0.05	1.64±0.12	2.31±0.08
120	—	—	—	2.66±0.08
150	—	5.82±0.13	2.30±0.17	2.76±0.08
170	—	—	2.26±0.10	—
200	—	—	2.46±0.06	3.39±0.10

Scheme 7

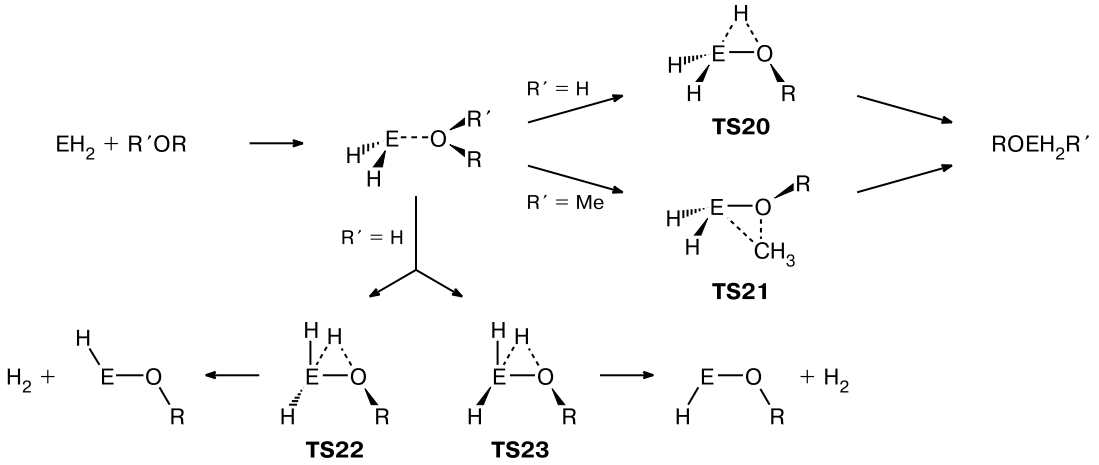

E = Si, Ge

methanol reacts faster than methanol itself, thus displaying the inverse isotope effect.[100] Comparison with the same reactions of SiH_2 [65,101,104] shows that GeH_2 is less reactive toward these O-donor molecules.[100] As has been discussed above, this decrease in reactivity on going from SiH_2 to GeH_2 was also observed in the addition and insertion reactions.

The temperature dependence of the rate constants for the GeH_2 reactions with these O-donor molecules has not been reported so far. Nevertheless, a negative temperature dependence is expected for all of them in the fall-off region,[100] based on the involvement of an intermediate complex predicted by quantum-chemical calculations.[66,103]

A quantum-chemical study of the PESs of the systems $GeH_2 + H_2O$, GeH_2 + MeOH, and $GeH_2 + Me_2O$ was performed at the MP2/6-311++G(d,p) level of theory.[66] Besides, the PESs of the systems $SiH_2 + H_2O$, SiH_2 + MeOH, SiH_2 + EtOH, $SiH_2 + CF_3OH$, and $SiH_2 + Me_2O$ were also studied in detail at this level and the PES of the system $SiH_2 + H_2O$ at the MP4(SDTQ)/6-311++G(d,p) and QCISD(T)/6-311++G(d,p) levels.[66] It was found that all the reactions studied start with formation of a quite stable pre-reaction complex with coordination of the O atom of the donor molecule to the Si or Ge atom of the carbene analog (Table 11). The possible routes of further transformations of the complexes are shown in Scheme 7.

The reaction channels connecting the complexes $R(H)O\cdots EH_2$ to HEOR + H_2 (E = Si, Ge) were revealed[66] for the first time. No similar channel was found for the complexes $Me_2O\cdot EH_2$ (E = Si, Ge). The only pathway for their further transformation consists of intramolecular insertion of the EH_2 submolecule into the C—O bond of the Me_2O fragment. Because the energy barrier to this reaction is quite high (Table 11), it is expected to stop at the step of complex formation under the temperature conditions of the kinetic experiments.[66]

Calculations[66] showed that the further reactions of the SiH_2 complexes with H_2O and alcohols have lower activation barriers and are more exothermic than the analogous reactions of the corresponding GeH_2 complexes. This is in agreement with the observation that SiH_2 is more reactive toward the O-donor molecules than GeH_2.[100] The complexes of GeH_2 with alcohols (ROH) and water have lower barriers to the H_2 elimination pathway to germylenes HGeOR than to the alternative pathway to the insertion products, H_3GeOR (see Table 11), despite

Table 11. Relative energies (ΔE + ZPE/kJ mol^{-1}) of the stationary points on the PES of the $EH_2 + H_2O$, EH_2 + MeOH and $EH_2 + Me_2O$ (E = Si, Ge) systems calculated[66] at the MP2/6-311++G(d,p) level

EH_2	R′OR	Complex	**TS20**	**TS21**	$ROEH_2R'$	**TS22**	*anti*-HEOR + H_2	**TS23**	*syn*-HEOR + H_2
GeH_2	H_2O	−46.1	84.4	—	−171.1	56.4	−69.2	56.5	−69.8
GeH_2	MeOH	−63.1	63.4	—	−179.2	38.0	−79.5	37.8	−81.8
GeH_2	MeOMe	−70.4	—	229.1	−230.9	—	—	—	—
SiH_2	H_2O	−53.3	38.5	—	−294.3	36.9	−112.1	38.3	−111.3
SiH_2	MeOH	−75.8	12.5	—	−304.1	14.9	−125.5	16.1	−128.1
SiH_2	MeOMe	−84.3	—	193.3	−365.1	—	—	—	—

the fact that the latter are much more stable. The corresponding SiH_2 complexes have barriers of comparable height to both types of transformations.[66]

Based on the results of quantum-chemical calculations,[66,103] the values of the high-pressure limiting rate constants were predicted[103] for the reactions of SiH_2 and GeH_2 with the O-donor species under consideration in the temperature range 100–1500 K using the activated-complex (transition state) theory. Unfortunately, the high-pressure limiting rate constants for these reactions could not be reliably estimated from the experiment.[100]

1.6. Thermochemical inferences

Some important thermochemical quantities can be obtained from the kinetic and quantum-chemical studies of the reactions of GeH_2 reviewed here. These are considered below.

Enthalpy of formation of GeH_2. The E_0 value obtained[35] for reaction (–8) after correction for thermal energy at 298 K is $E_a(-8) = 158$ kJ mol^{-1}. Then, the enthalpy change $\Delta H°(-8,8) = E_a(-8) - E_a(8) + RT$ is equal to 165.7 kJ mol^{-1} with an uncertainty of ±12 kJ mol^{-1} transferred from that of E_0 coming from RRKM modeling. Combining $\Delta H°(-8,8)$ with the literature values[105] of $\Delta H°_f(GeH_4) = 90.4\pm2.1$ kJ mol^{-1} and $\Delta H°_f(Ge_2H_6) = 161.9\pm1.3$ kJ mol^{-1} leads to $\Delta H°_f(GeH_2) = 237.2\pm12$ kJ mol^{-1}. Similarly, the value of 233.0±12 kJ mol^{-1} for $\Delta H°_f(GeH_2)$ was derived[50] from E_0 obtained for reaction (–9) using $\Delta H°_f(SiH_4)$[63] = 34.3±2.1 kJ mol^{-1} and $\Delta H°_f(H_3SiGeH_3) = 120\pm3$ kJ mol^{-1} (recalculated[50] value based on earlier measurements[106]).

There are several previous estimates of $\Delta H°_f(GeH_2)$, based on experimental data, *viz.*, 238±12,[107,108] 255±42,[34] and >248 kJ mol^{-1} (more probably, 258 kJ mol^{-1}).[109] All these values are in reasonable agreement with those derived from the E_0 values for reactions (–8) and (–9), although the latter are more substantiated. They are also in good agreement with the values of 252,[35] 250,[39] and 239 and 235 kJ mol^{-1} [50] based on the results of quantum-chemical calculations.

Divalent State Stabilization Energy of GeH_2. A very useful reactivity index of carbene analogs is the Divalent State Stabilization Energy (*DSSE*).[62,63] For GeH_2, it is defined as follows:

$$E_{DSSE}(GeH_2) = D(H_3Ge{-}H) - D(H_2Ge{-}H) =$$

$$= 2\Delta H°_f(GeH_3) - \Delta H°_f(GeH_4) - \Delta H°_f(GeH_2).$$

The use of $\Delta H°_f(GeH_2)$ in combination with the known $\Delta H°_f(GeH_3)$ and $\Delta H°_f(GeH_4)$ values yields $DSSE(GeH_2) = 119$ kJ mol^{-1} (with uncertainties probably amounting to ±20 kJ mol^{-1}).[35] This value is greater than the figure of 94±4 kJ mol^{-1} for $DSSE(SiH_2)$.[63] Thus, the *DSSE* increases on going down Group 14, a phenomenon that has long been known as the "Inert Pair Effect".[110]

The strain energy in germirane. From the values for $\Delta H°_f(C_2H_4) = 52.3$ kJ mol^{-1} [111] and $\Delta H°_f(GeH_2) = 237$ kJ mol^{-1} [35] (see above), the G2 calculations[72] (Fig. 4) lead to $\Delta H°_f$(germirane) = 195 kJ mol^{-1}. An estimate of the enthalpy of formation of strain-free germirane based on an organogermanium additivity scheme gave 48 kJ mol^{-1}.[72] Therefore, the strain energy of germirane is *ca.* 147 kJ mol^{-1}. The strain energy obtained for silirane from experimental data is *ca.* 167 kJ mol^{-1}.[76] Thus, despite the fact that silirane is much more stable than germirane ($\Delta H°$ for the decomposition of silirane into $SiH_2 + C_2H_4$ is 201 kJ mol^{-1},[76] while the corresponding value for germirane is 94 kJ mol^{-1} [72]), it has a slightly higher strain energy. Lower stability of germirane compared to silirane with respect to dissociation is largely due to the weakness of Ge—C(sp^3) bonds compared to Si—C(sp^3) bonds. Although slightly differing estimates of strain energy may be obtained from other theoretical calculations,[84–86,89,112] this conclusion is not altered.

Because of the two-channel nature of the process $GeH_2 + C_2H_4$, a thermochemical estimate of ΔH_f^0(germirane) cannot be made from the kinetic data and RRKM fits.[72] Obviously, this also applies to 2-methylgermirane, for which such an estimate was made based on the wrong assumption that the reaction $GeH_2 + C_3H_6$ had a single channel.[74]

The strain energy in germirene. From the values for $\Delta H°_f(C_2H_2) = 227$ kJ mol^{-1} [111] and $\Delta H°_f(GeH_2) = 237$ kJ mol^{-1} [35], the G2 calculations[75] give $\Delta H°_f$(germirene) = 356 (or 357) kJ mol^{-1}. From an estimate of 157 kJ mol^{-1} for strain-free germirene[75] based on the organogermanium additivity scheme, the strain energy of germirene is *ca.* 200 kJ mol^{-1}. A comparison with silirene (for which the strain energy is *ca.* 222 kJ mol^{-1} and the enthalpy of decomposition into $SiH_2 + C_2H_2$ is 289 kJ mol^{-1} [80,113] shows that while silirene is much more stable it has a slightly higher strain energy. Thus, the lower stability of germirene compared to silirene toward dissociation is largely due to the weakness of Ge—C(sp^2) bonds compared to Si—C(sp^2) bonds. This conclusion is analogous to that drawn above for germirane and silirane. It is not altered by use of the data of other theoretical calculations of the SiC_2H_4 potential energy surface.[95,96]

Divalent State Stabilization Energy in dimethylgermylene. Using $\Delta H°_f(C_2H_4) = 52.3$ kJ mol^{-1} [111] and $\Delta H°_f(GeH_2) = 237$ kJ mol^{-1} [35] (see above), the G2 calculations[72] (Fig. 4) lead to $\Delta H°_f(Me_2Ge) = 138$ kJ mol^{-1}. The divalent state stabilization energy of $GeMe_2$ is defined as follows:

$$E_{DSSE}(GeMe_2) = D(Me_3Ge{-}Me) - D(Me_2Ge{-}Me) =$$

$$= 2\Delta H_f^0(GeMe_3) - \Delta H_f^0(GeMe_4) - \Delta H_f^0(GeMe_2).$$

Assuming a value of 81 kJ mol^{-1} for $\Delta H^\circ_f(GeMe_3)$, based on the experimental measurement of $D(Me_3Ge-H)$,[114] and taking into account $\Delta H^\circ_f(GeMe_4) = -102.5$ kJ mol^{-1},[115] the *DSSE*($GeMe_2$) is derived as 126 kJ mol^{-1} with an expected uncertainty of ±20 kJ mol^{-1}.[72] An analogous estimate of *DSSE*(GeMeH) gave a value of 111±20 kJ mol^{-1}.[72] Thus, the trend of increasing *DSSE* value with methyl substitution found for silylenes (*DSSE*(SiH_2) = 94±4,[63] *DSSE*(SiHMe) = 113±11,[63] *DSSE*($SiMe_2$) = 128±11 [63]) is not reproduced for germylenes (*DSSE*(GeH_2) = 119±20,[35] *DSSE*(GeHMe) = 111±20 and *DSSE*($GeMe_2$) = 126±20 [72]), although this could be hidden in the uncertainties.

2. Kinetics and mechanisms of reactions of dimethylstannylene

The chemistry of labile organostannylenes has been explored to a much lesser extent than the chemistry of labile silylenes and germylenes. It has been shown by end product analysis that in the presence of many potential reagents, which silylene and germylene readily react with, stannylenes like $SnMe_2$ simply polymerize.[4] This suggests that stannylenes are much less reactive than silylenes and germylenes. To the best of our knowledge, there have been no published kinetic studies of reactions of labile stannylenes prior to our work. Thus, quantitative comparison of the reactivity of stannylenes with those of silylenes and germylenes was impossible up to now. Recently, however, we succeeded in generating dimethylstannylene $SnMe_2$, which may reasonably be regarded as the prototype organostannylene, by laser flash photolysis at 193 nm in the gas-phase. This was accomplished using several precursors, and room-temperature kinetic studies for some of its reactions were performed.[116]

2.1. Generation and identification of $SnMe_2$

The experimental technique used in the kinetic studies of reactions of $SnMe_2$[116] was the same as in the studies reactions of of GeH_2 and $GeMe_2$. Because pentamethyldistannane and 1,1-dimethyl-1-stannacyclopent-3-ene, tin analogs of convenient photoprecursors of $SiMe_2$ [10] and $GeMe_2$ [25], were unavailable, a number of other potential photoprecursors of $SnMe_2$ were tested. These included $SnMe_4$, Sn_2Me_6, Me_3SnH, and $PhSnMe_2H$, all possessing strong UV absorptions at 193 nm.[116]

Laser flash photolysis of all these precursors at 193 nm gave transient species characterized by a very similar broad UV band with a maximum at *ca*. 515 nm. For two of the precursors, *viz*., Sn_2Me_6 and $PhSnMe_2H$, stronger absorptions at shorter wavelengths (<480 nm) were observed, suggesting that other intermediates absorbing in this region were present. The yields of the transient species varied depending on the precursor. Under the same experimental conditions, the most intense signals were detected when Sn_2Me_6 and $PhSnMe_2H$ were used as precursors, while Me_3SnH gave the weakest signal.

The UV spectrum of $SnMe_2$ in the gas phase or other phases has not been reported so far. Nevertheless, a transient species with the absorption maximum at 514 nm can be reliably identified as $SnMe_2$. First of all, four tin compounds of different structure gave the same spectrum of the transient species. Because the only common fragment of these compounds is the $SnMe_2$ fragment, one can conclude that it is this structure that can be ascribed to the transient species. The available data on the absorption maxima of structurally similar stable stannylenes and germylenes[7] indicate that for alkyl-substituted species the spectra of stannylenes are red shifted relative to those of germylenes by several tens of nm. Because the gas-phase UV band corresponding to the $S_0 \rightarrow S_1$ transition of $GeMe_2$ has a maximum at 476 nm,[25] the band of the same transition of $SnMe_2$ is expected at around 520 nm. Our quantum-chemical calculations by the CIS and TD DFT B3LYP methods also predicted the lowest vertical transition for $SnMe_2$ to lie around 520 nm.[116] A prior check showed that these methods reproduced well the known energies of the lowest vertical electronic transitions for $SiMe_2$ and $GeMe_2$.[116]

Further additional evidence in favor of our identification of the transient species was obtained from GLC analysis of the stable end products of photodecomposition of these precursors both in the presence and in the absence of O_2, a known radical scavenger.The following pathways of decomposition of precursors were proposed based on the results obtained:

$$SnMe_4 \xrightarrow{i} SnMe_2 + C_2H_6\ (\sim 90\%) \quad (18)$$

$$Sn_2Me_6 \xrightarrow{i} SnMe_2 + SnMe_4\ (\sim 25\%) \quad (19a)$$

$$Sn_2Me_6 \xrightarrow{i} Sn_2Me_4 + C_2H_6\ (\sim 50\%) \quad (19b)$$

$$Me_3SnH \xrightarrow{i} SnMe_2 + CH_4\ (\sim 40\%) \quad (20a)$$

$$Me_3SnH \xrightarrow{i} SnHMe + C_2H_6\ (\sim 50\%) \quad (20b)$$

$$PhSnMe_2H \xrightarrow{i} SnMe_2 + C_6H_6\ (\sim 30\%) \quad (21a)$$

$$PhSnMe_2H \xrightarrow{i} SnMePh + CH_4\ (\sim 30\%) \quad (21b)$$

$$PhSnMe_2H \xrightarrow{i} SnHPh + C_2H_6\ (\sim 30\%) \quad (21c)$$

i. *h*ν, 193 nm.

In summary, both the wavelength of the maximum in the spectrum of the transient species and its formation from different precursors provide strong evidence that

elimination of $SnMe_2$ is the major route of photodecomposition of all these precursors. Thus, $SnMe_2$ was generated in the gas phase for the first time and characterized by its UV band corresponding to the lowest S—S transition.

2.2. First absolute rate constants for reactions of $SnMe_2$ in the gas phase at room temperature

The set of substrates for kinetic measurements[116] was chosen to cover a selection of potential $SnMe_2$ reaction types. Kinetic measurements were performed in SF_6 bath gas, using $SnMe_4$ as the most selective precursor.[116] The total pressure in the reaction systems was kept at 5 or 10 Torr. No overall pressure dependence was investigated for any of the reactions. $SnMe_2$ was monitored at 501.7 and 514.5 nm, in the strongest absorption region. The rate constants obtained are presented in Table 12. The uncertainties for the reaction rate constants are single standard deviations. No reactions were found with C_3H_8 (10 Torr), Me_3SiH (10 Torr), GeH_4 (10 Torr), Me_2GeH_2 (10 Torr), C_2H_4 (30 Torr), and N_2O (10 Torr). The lack of reactions was used to put upper limits for the rate constants (see Table 12). $SnMe_2$ reacted with buta-1,3-diene, MeC≡CMe, MeOH, HCl, C_4H_9Br, and SO_2. These findings are consistent with what is already known from end product studies in solution.[4] In addition to these, the reaction of $SnMe_2$ with O_2 was also studied, but a linear second-order plot for k_{obs} was not obtained. If there is a second-order reaction, it has a rate constant somewhere in the range $(0.4–1.7)\cdot10^{-11}$ cm^3 molecule^{-1} s^{-1}.[116]

The observed lack of reactivity of $SnMe_2$ with respect to several substrates that previously have been found to react with silylenes and germylenes is not too surprising. As was discussed earlier, the heavy carbene analogs seem to get less reactive with an increase in the atomic number of the central atom, *i.e.*, germylenes are less reactive than silylenes. Methyl substituents additionally decrease the reactivity of heavy carbene analogs. Thus, the results obtained show that this trend holds on going further to dimethylstannylene (Table 13).

As far as insertion processes are concerned, $SiMe_2$ and $GeMe_2$ insert fairly slowly into Si—H and Ge—H bonds (see Table 13). Moreover, from the studies of SiH_2 and GeH_2 (see above) it is clear that the reactivity is strongly affected by the strength of the substrate bond for insertion. Namely, insertion of GeH_2 into the Si—H bond is considerably slower than insertion of SiH_2 into the Ge—H bond (see Table 4). Hence, one can expect that $SnMe_2$ is unlikely to insert easily into any E—H bond stronger than Sn—H, and taking into account the sluggishness of insertion of $GeMe_2$ into the Ge—H bond (see Table 13), even this is likely to be very slow.

The lack of reaction of $SnMe_2$ with ethylene is probably associated with a decrease in stability of heterocyclopropanes *cyclo*-$EH_2CH_2CH_2$ on going down the Group 14 elements, which has been demonstrated by comparing the enthalpies of additions of EH_2 to C_2H_4[72,76] for E = Si and Ge (see above). There are no published data on the stability of stannirane. However, the results of MP2/3-21G(d)//RHF/3-21G(d) calculations of stannirene[113] show that this ring, although highly strained, is 52 kJ mol^{-1} more favorable than the starting SnH_2 + C_2H_2. This could explain the fact that $SnMe_2$ reacts with MeC≡CMe. Nevertheless, the measured rate constant[116] for this reaction seems surprisingly high and inconsistent with the predicted[113] small energy gain for the addition of SnH_2 to HC≡CH to form stannirene. Synthesis of the only stable stannirene was reported starting from a stable stannylene and a highly strained acetylene, 3,3,6,6-tetramethyl-1-thiacyclohept-4-yne.[117]

1,3-Dienes are known to be efficient trapping agents for silylenes and germylenes.[3,4] Despite this fact, trapping of $SnMe_2$ with 2,3-dimethylbuta-1,3-diene and a number of other dienes failed.[4] It was shown, however, that stable Lappert´s dialkylstannylene adds smoothly to these 1,3-dienes.[118] This implies that stannylenes are reactive with respect to 1,3-dienes, although the products can be unstable. Our measurements support this suggestion. The

Table 12. Gas-phase rate constants (k/cm^3 molecule^{-1} s^{-1}) for reactions of $SnMe_2$ at 296±2 K [116]

Substrate	k	Substrate	k
1,3-C_4H_6	$(5.97\pm0.17)\cdot10^{-11}$	C_3H_8	$\le3.1\cdot10^{-14}$
MeC≡CMe	$(7.84\pm0.12)\cdot10^{-12}$	Me_3SiH	$\le6.2\cdot10^{-14}$
MeOH	$(2.60\pm0.10)\cdot10^{-12}$	GeH_4	$\le3.1\cdot10^{-14}$
HCl	$(8.08\pm0.35)\cdot10^{-13}$	Me_2GeH_2	$\le9.3\cdot10^{-14}$
Bu^nBr	$(2.88\pm0.28)\cdot10^{-12}$	C_2H_4	$\le1.0\cdot10^{-14}$
SO_2	$(3.35\pm0.12)\cdot10^{-11}$	N_2O	$\le9.3\cdot10^{-14}$

Table 13. Comparison of rate constants (k/cm^3 molecule^{-1} s^{-1}) for gas-phase reactions of $SiMe_2$, $GeMe_2$, and $SnMe_2$ at room temperature[a]

Substrate	$SiMe_2$ [10]	$GeMe_2$ [25]	$SnMe_2$ [116]
1,3-C_4H_6	$7.5\cdot10^{-11}$	$1.1\cdot10^{-11}$	$6.0\cdot10^{-11}$
Alkyne[b]	$4.6\cdot10^{-11}$	$1.3\cdot10^{-11}$	$7.8\cdot10^{-12}$
Alkene[c]	$3.7\cdot10^{-11}$	$1.3\cdot10^{-11}$	$\le1.0\cdot10^{-14}$
Me_2GeH_2	—	$2.3\cdot10^{-13}$ [d]	$\le9.3\cdot10^{-14}$
Me_3SiH	$4.5\cdot10^{-12}$	$<6\cdot10^{-15}$	$\le6.2\cdot10^{-14}$
Alkane[e]	$<5\cdot10^{-14}$	$<2\cdot10^{-14}$	$\le3.1\cdot10^{-14}$
O_2	$2.5\cdot10^{-13}$	$4.5\cdot10^{-14}$	$(0.4–1.7)\cdot10^{-11}$

[a] For known pressure-dependent reactions, the high-pressure limiting values are listed.
[b] C_2H_2 ($SiMe_2$ and $GeMe_2$) and MeC≡CMe ($SnMe_2$).
[c] C_3H_6 ($SiMe_2$), $Me_3CCH{=}CH_2$ ($GeMe_2$), and C_2H_4 ($SnMe_2$).
[d] See Ref. 26 and Table 2.
[e] Me_4Si ($SiMe_2$) and C_3H_8 ($GeMe_2$ and $SnMe_2$).

rate constant for the reaction of $SnMe_2$ with buta-1,3-diene is the largest of the measured rate constants (Table 12), which shows the efficiency of 1,3-dienes as trapping agents for stannylenes.

The observation of reactions of $SnMe_2$ with HCl and BuBr[116] is consistent with the known affinity of Lappert´s dialkylstannylene with halides,[118] despite the fact that the solution studies did not establish conclusively the involvement of free labile stannylenes in the formation of C—Hal insertion products.[4] At least two possible mechanisms of these insertion processes were suggested.[4] These are a concerted mechanism and that with halogen abstraction by the stannylene with formation of free radicals. Thermochemical considerations show that in the gas phase the latter mechanism may be at best marginal.[116]

The reversibility of reactions of heavy carbene analogs with MeOH is an issue. This is the case in the reactions of GeH_2 and SiH_2 with MeOH discussed in the previous section. There was no evidence of reversibility in the reaction $SnMe_2$ + MeOH at room temperature.[116] An earlier kinetic study of the reaction of $SiMe_2$ with MeOH also showed irreversibility of the formation of the donor-acceptor complex as the first step at room temperature.[64] However, reversibility would be expected for $SiMe_2$ at higher temperatures by analogy with the reactions of SiH_2 [101] and GeH_2 [119] with MeOH.

Concerning the reactions of $SnMe_2$ with SO_2 and N_2O, the first step may be reasonably expected to be O-atom transfer. However, thermochemical considerations showed[116] that in this case reaction with N_2O should be possible, while that with SO_2 is not, which contradicts the experimental data. Thus, this latter reaction at least, must proceed by some other pathway.

The rate constants obtained for different types of reactions of EMe_2 (E = Si, Ge, Sn) are compared in Table 13. Although the number of data is extremely limited, the general decrease in reactivity on going from $SiMe_2$ to $SnMe_2$ is clear. Nevertheless, $SnMe_2$ is still a very reactive species, reacting with $H_2C{=}CHCH{=}CH_2$ and MeC≡CMe at rates of approximately an order of magnitude lower than the collisional limit only. Following trends in the reactivity of heavy carbene analogs in detail requires the investigation of the temperature dependence of $SnMe_2$ kinetics. Such studies are in progress now.

Conclusion

The studies surveyed here conclusively demonstrate that the pattern of the reactivity of germylenes (and probably stannylenes) is very similar to that of silylenes. All these species are reactive with respect to the same reagent types, react with them at comparable (often, very high) rates, and the mechanisms of these reactions are much the same. Despite the fact that reactions of carbene analogs are often written as elementary reactions in many transformations of organoelement compounds of the Group 14 elements, these reactions are not simple and often involve several steps. Very often the first step of germylene and silylene reactions is the formation of a pre-reaction complex between the carbene analog and the reagent where the carbene analog acts as a Lewis acid. Due to the reversibility of this electrophilic step, in many cases a negative activation energy for the overall reaction is observed. All the reactions of germylenes, whose activation parameters have been obtained to date, are characterized by negative activation energies.

The kinetic studies of germylene and stannylene reactions allowed us to trace a trend in the reactivity among the different classes of heavy carbene analogs on a quantitative basis for the first time. It has been shown that the reactivity decreases on going from silylenes to stannylenes. However, the decrease is not very strong for the carbene analogs with the same substituents. The rate constants for their reactions with the same reagents differ usually by at most an order of magnitude, as can be concluded from the available data. This conclusion may seem to be in contradiction with the impression obtained from solution studies by end product analysis, which suggests a stronger decrease in reactivity in this series. However, our findings from quantum-chemical calculations indicate that in some reactions the end products are reactive intermediates themselves. Thus, a likely explanation for this discrepancy may consist of a larger branching of the overall reaction channels on going from silylenes to the heavier carbene analogs, making very risky an assessment of the reactivity based on the analysis of a single target final product. This can be inferred from a comparison of the PESs for the reactions of SiH_2 and GeH_2 with ethylene and acetylene.

As can be seen from the above discussion, time-resolved studies in combination with quantum-chemical calculations represent a powerful tool for the investigation of reaction mechanisms of labile species. The application of this tool to the study of germylene reactions is well underway but for stannylene reactions it has only just begun and a lot remains to be done. However, a better understanding of the chemistry of these important intermediates is beginning to emerge.

This work was carried out with the financial support from the Russian Foundation for Basic Research (Project Nos 03-03-32564 and 04-03-32838), the Ministry of Education and Science of the Russian Federation (in the framework of the Federal Target Research and Technological Program "Research and Development on Priority Avenues of Science and Technology"), the Russian Federation Presidential Foundation (in the framework of the Program for Support of Leading Research Schools (Grant NSh-1987.2003.3), the Russian Academy of Sciences

(Chemistry and Materials Science Division, in the framework of the Program "Theoretical and Experimental Study of Chemical Bonding and Mechanisms of Chemical Reactions and Processes"; and the Presidium of the Russian Academy of Sciences, in the framework of the Program "Thermal Physics and Mechanics of Intense Energy Actions"), the DGI of the Ministerio de Ciencia y Tecnologia (Spain, Project BQU2002-03381), and the NATO (project PST.CLG.975368).

References

1. O. M. Nefedov and M. N. Manakow, *Angew. Chem*., 1966, **78**, 1966.
2. O. M. Nefedov, A. I. Ioffe, and L. G. Menchikov, *Chemistry of Carbenes*, Moscow, Khimiya, 1990.
3. P. P. Gaspar and R. West, in *The chemistry of organic silicon compounds*, Eds Z. Rappoport and Y. Apeloig, J. Wiley and Sons Ltd, Chichester, V. 2, 1998, 2463.
4. W. P. Neumann, *Chem. Rev*, 1991, **91**, 311.
5. M. P. Egorov and P. P. Gaspar, *Germanium, organometallic chemistry, the encyclopedia of inorganic chemistry*, Ed. R. B. King, J. Wiley and Sons, New York, 1995, **3**, 1229.
6. O. M. Nefedov, M. P. Egorov, A. I. Ioffe, L. G. Menchikov, P. S. Zuev, V. I. Minkin, B. Ya. Simkin, and M. N. Glukhovtsev, *Pure Appl. Chem*., 1992, **64**, 265.
7. S. E. Boganov; M. P. Egorov, V. I. Faustov, and O. M. Nefedov, in *The chemistry of organic germanium, tin and lead compounds*, Ed. Z. Rappoport, Wiley, 2002, V. 2, Part 1, 749.
8. I. Safarik, V. Sandhu, E. M. Lown, O. P. Strausz, and T. N. Bell, *Research on Chem. Intermediates*., 1990, **14**, 105.
9. J. M. Jasinski, R. Becerra, and R. Walsh, *Chem. Rev.*, 1995, **95**, 1203
10. R. Becerra and R. Walsh, in *Research in Chemical Kinetics*, Eds R. G. Compton and G. Hancock, Elsevier, Amsterdam, 1995, V. 3, p. 263.
11. M. P. Egorov, A. S. Dvornikov, V. A. Kuzmin, S. P. Kolesnikov, and O. M. Nefedov, *Izv. Akad. Nauk SSSR, Ser. Khim*., 1987, 1200 [*Bull. Acad. Sci. USSR, Div. Chem. Sci.*, 1987, **36**, 1114 (Engl. Transl.)].
12. K. Mochida, M. Wakasa, Y. Nakadira, Y. Sakaguchi, and H. Hayashi, *Organometallics*, 1988, **7**, 1869.
13. S. P. Kolesnikov, M. P. Egorov, A. S. Dvornikov, V. A. Kuzmin, and O. M. Nefedov, *Metalloorg. Khim*., 1989, **2**, 799 [*Organomet. Chem. USSR*, 1989, **2** (Engl. Transl.)].
14. M. Wakasa, I. Yoneda, and K. Mochida, *J. Organometal. Chem*., 1989, **366**, C1.
15. K. Mochida, I. Yoneda, and M. Wakasa, *J. Organometal. Chem*., 1990, **399**, 53.
16. K. L. Bobbitt, V. M. Maloney, and P. P. Gaspar, *Organometallics*, 1991, **10**, 2772.
17. K. Mochida, N. Kanno, R. Kato, M. Kotani, S. Yamauchi, M. Wakasa, and H. Hayasi, *J. Organometal. Chem*., 1991, **415**, 191.
18. K. Mochida and S. Tokura, *Bull. Chem. Soc. Jpn*., 1992, **65**, 1642.
19. K. Mochida, K. Kimijima, H. Chiba, M. Wakasa, and H. Hiyashi, *Organometallics*, 1994, **13**, 404.
20. S. Konieczny, S. J. Jacobs, J. K. Wilking, and P. P. Gaspar, *J. Organometal. Chem*., 1988, **341**, C17.
21. N. P. Toltl, W. J. Leigh, G. M. Kollegger, W. G. Stibbs, and K. M. Baines, *Organometallics*, 1996, **15**, 3732.
22. K. Mochida, S. Tokura, and S. Murata, *J. Chem. Soc., Chem. Comm*., 1992, 250.
23. R. Becerra, S. E. Boganov, M. P. Egorov, O. M. Nefedov, and R. Walsh, *Chem. Phys. Lett.*, 1996, **260**, 433.
24. U. A. Alexander, N. A. Trout, K. D. King, and W. D. Lawrance, *Chem. Phys. Lett.*, 1999, **299**, 291.
25. R. Becerra, S. E. Boganov, M. P. Egorov, V. Ya. Lee, O. M. Nefedov, and R. Walsh, *Chem. Phys. Lett.*, 1996, **250**, 111.
26. R. Becerra, M. P. Egorov, I. V. Krylova, O. M. Nefedov, and R. Walsh, *Chem. Phys. Lett.*, 2002, **351**, 47.
27. J. E. Baggott, M. A. Blitz, H. M. Frey, P. D. Lightfoot, and R. Walsh, *Chem. Phys. Lett.*, 1987, **135**, 39.
28. E. C.-L. Ma, D. P. Paquin, and P. P. Gaspar, *J. Chem. Soc., Chem. Comm*., 1980, 381.
29. E. C.-L. Ma, K. Kobayashi, M. W. Barzilai, and P. P. Gaspar, *J. Organomet. Chem*., 1982, **224**, C13.
30. D. Lei and P. P. Gaspar, *Polyhedron*, 1991, **10**, 1221.
31. W. Du, L. A. Keeling, and C. M. Greenlief, *J. Vac. Sci. Technol. A*, 1994, **12**, 2281.
32. C. Isobe, H.Cho, and J. E. Crowell, *Surf. Sci.*, 1993, **295**, 117.
33. H. Simka, M. Hierlemann, M. Utz, and K. F. Jensen, *J. Electrochem. Soc.*, 1996, **143**, 2646.
34. C. G. Newman, J. Dzarnoski, M. A. Ring, and H. E. O´Neal, *Int. J. Chem. Kinet.*, 1980, **12**, 661.
35. R. Becerra, S. E. Boganov, M. P. Egorov, V. I. Faustov, O. M. Nefedov, and R. Walsh, *J. Am. Chem. Soc.*, 1998, **120**, 12657.
36. K. Saito and K. Obi, *Chem. Phys. Lett.*, 1993, **215**, 193.
37. K. Obi, M. Fukushima, and K. Saito, *Appl. Surf. Sci.*, 1994, **79/80**, 465.
38. K.Saito and K. Obi, *Chem. Phys.*, 1994, **187**, 381.
39. J. Karolczak, W. P. Harper, R. S. Grev, and D. J. Clouthier, *J. Chem. Phys.*, 1995, **103**, 2839.
40. A. Campargue and R. Escribano, *Chem. Phys. Lett.*, 1999, **315**, 397.
41. W. J. Leigh, C. R. Harrington, and I. Vargas-Baca, *J. Am. Chem. Soc.*, 2004, **126**, 16105.
42. J. M. Jasinski, B. S. Meyerson, and B. A. Scott, *Annu. Rev. Phys. Chem*., 1987, **38**, 109.
43. G. Lu and J. E. Crowell, *J. Chem. Phys.*, 1993, **98**, 3415.
44. P. P. Gaspar, C. A. Levy, J. J. Frost, and S. A. Bock, *J. Am. Chem. Soc.*, 1969, **91**, 1573.
45. P. Estacio, M. D. Sefcik, E. K. Chan, and M. A. Ring, *Inorg. Chem.*, 1970, **9**, 1068.
46. M. D. Sefcik and M. A. Ring, *J. Organomet. Chem.*, 1973, **59**, 167.
47. R. Becerra, I. V. Krylova, M. P. Egorov, O. M. Nefedov and R. Walsh, *VII Conf. "Chemistry of Carbenes and Related Intermediates" (Kazan, June 23—26, 2003)*, Abstrs, Kazan, 2003, p. 73.
48. J. E. Baggott, M. A. Blitz, H. M. Frey, and R. Walsh, *J. Am. Chem. Soc.*, 1990, **112**, 8337.
49. J. E. Baggott, H. M. Frey, P. D. Lightfoot, R. Walsh, and I. M. Watts, *J. Chem. Soc., Faraday Trans.*, 1990, **86**, 27.

50. R. Becerra, S. E. Boganov, M. P. Egorov, V. I. Faustov, O. M. Nefedov, and R. Walsh, *Phys. Chem. Chem. Phys.*, 2001, **3**, 184.
51. R. Becerra, S. E. Boganov, M. P. Egorov, O. M. Nefedov, and R. Walsh, *Mendeleev Commun.*, 1997, 87.
52. R. Becerra and R. Walsh, *Phys. Chem. Chem. Phys.*, 1999, **1**, 5301.
53. U. N. Alexander, K. D. King, and W. D. Lawrance, *Chem. Phys. Lett.*, 2000, **319**, 529.
54. R. Becerra, H. M. Frey, B. P. Mason, R. Walsh, and M. S. Gordon, *J. Chem. Soc., Faraday Trans.*, 1995, **91**, 2723.
55. R. Becerra, S. Boganov, and R. Walsh, *J. Chem. Soc., Faraday Trans.*, 1998, **94**, 3569.
56. I. W. Carpenter, *PhD Thesis*, University of Reading, 1996.
57. J. Troe, *J. Chem. Soc., Faraday Trans.*, 1994, **90**, 2303.
58. G. Trinquier, *J. Chem. Soc., Faraday Trans.*, 1993, **89**, 775.
59. R. Becerra, H. M. Frey, B. P. Mason, and R. Walsh, *J. Chem. Soc., Faraday Trans.*, 1993, **89**, 411.
60. P. N. Noble and R. Walsh, *Int. J. Chem. Kinet.*, 1983, **15**, 547.
61. R. Becerra and R. Walsh, *Int. J. Chem. Kinet.*, 1999, **31**, 393.
62. R. Walsh, *Pure Appl. Chem.*, 1987, **59**, 69.
63. R. Becerra and R. Walsh, *Thermochemistry*, in *The Chemistry of Organosilicon Compounds,* Eds Z. Rappoport and Y. Apeloig, Wiley, Chichester, 1998, V. **2**, Chapt. 4, p. 153.
64. J. E. Baggott, M. A. Blitz, H. M. Frey, P. D. Lightfoot, and R. Walsh, *Int. J. Chem. Kinet.*, 1992, **24**, 127.
65. U. N. Alexander, K. D. King, and W. D. Lawrance, *Phys. Chem. Chem. Phys.*, 2001, **3**, 3085.
66. M. W. Heaven, G. F. Metha, and M. A. Buntine, *J. Phys. Chem., A*, 2001, **105**, 1185.
67. S. Su and M. S. Gordon, *Chem. Phys. Lett.*, 1993, **204**, 306.
68. R. Becerra, S. E. Boganov, M. P. Egorov, V. I. Faustov, O. M. Nefedov, and R. Walsh, *Can. J. Chem.*, 2000, **78**, 1428.
69. J. M. Jasinski, *J. Phys. Chem.*, 1986, **90**, 555.
70. M. S. Gordon, D. R. Gano, J. S. Binkley, and M. J. Frisch, *J. Am. Chem. Soc.*, 1986, **108**, 2191.
71. R. L. Jenkins, R. A. Kedrowski, L. E. Elliot, D. C. Tappen, D. J. Schlyer, and M. A. Ring, *J. Organomet. Chem.*, 1975, **86**, 347.
72. R. Becerra, S. E. Boganov, M. P. Egorov, V. I. Faustov, V. M. Promyslov, O. M. Nefedov, and R. Walsh, *Phys. Chem. Chem. Phys.*, 2002, **4**, 5079.
73. R. Becerra and R. Walsh, *Phys. Chem. Chem. Phys.*, 2002, **4**, 6001.
74. R. Becerra and R.Walsh, *J. Organomet. Chem.*, 2001, **636**, 49.
75. R. Becerra, S. E. Boganov, M. P. Egorov, V. I. Faustov, I. V. Krylova, O. M. Nefedov, V. M. Promyslov, and R. Walsh, *Phys. Chem. Chem. Phys.*, 2004, **6**, 3370.
76. N. Al-Rubaiey and R. Walsh, *J. Phys. Chem.*, 1994, **98**, 5303.
77. N. Al-Rubaiey, R. Becerra, and R. Walsh, *Phys. Chem. Chem. Phys.*, 2002, **4**, 5072.
78. N. Al-Rubaiey, I. W. Carpenter, R. Walsh, R. Becerra, and M. S. Gordon, *J. Phys. Chem., A*, 1998, **102**, 8564.
79. R. Becerra, H. M. Frey, B. P. Mason, and R. Walsh, *J. Chem. Soc., Chem. Commun.*, 1993, 1050.
80. R. Becerra and R. Walsh, *Int. J. Chem. Kinet.*, 1994, **26**, 45.
81. R. Becerra, J. P. Cannady, and R. Walsh, *Phys. Chem. Chem. Phys.*, 2001, **3**, 2343.
82. R. Becerra, J. P. Cannady, and R. Walsh, *J. Chem. Phys A.*, 2002, **106**, 11558.
83. P. Antoniotti, P Benzi, M. Castiglioni, and P. Volpe, *Eur. J. Inorg. Chem.* 1999, 323.
84. S. Sakai, *Int. J. Quantum Chem.*, 1998, **70**, 291.
85. M.-D. Su and S.-Y. Chu, *J. Am. Chem. Soc.*, 1999, **121**, 11478.
86. D. A. Horner, R. S. Grev, and H. F. Schaefer III, *J. Am. Chem. Soc.*, 1992, **114**, 2093.
87. W. Ando, H. Ohgaki, and Y. Kabe, *Angew. Chem. Int. Ed. Engl.*, 1994, **33**, 659.
88. H. Ohgaki, Y. Kabe, and W. Ando, *Organometallics*, 1995, **14**, 2139.
89. P. N. Skancke, D. A. Hrovat, and W. T. Borden, *J. Am. Chem. Soc.*, 1997, **119**, 8012.
90. V. N. Khabashesku, K. N. Kudin, J. Tamas, S. E. Boganov, J. L. Margrave, and O. M. Nefedov, *J. Am. Chem. Soc.*, 1998, **120**, 5005.
91. V. N. Khabashesku, S. E. Boganov, K. N. Kudin, J. L. Margrave, J. Michl, and O. M. Nefedov, *Russ. Chem. Bull.*, 1999, **48**, 2003.
92. F. Anwari and M. S. Gordon, *Isr. J. Chem.*, 1983, **23**, 129.
93. A. D. Krebs and J. Berndt, *Tetrahedron Lett.*, 1983, **24**, 4083.
94. M. P. Egorov, S. P. Kolesnikov, Yu. T. Struchkov, M. Yu. Antipin, S. V. Sereda, and O. M. Nefedov, *J. Organometal. Chem.*, 1985, **290**, C27.
95. M. T. Nguyen, D. Sengupta, and L. G. Vanquickenborne, *Chem. Phys. Lett.*, 1995, **240**, 513.
96. P. N. Skancke, D. A. Hrovat, and W. T. Borden, *J. Phys. Chem. A*, 1999, **103**, 4043.
97. G. Maier, H. P. Reisenauer, and H. Egenolf, *Eur. J. Org. Chem.*, 1998, 1313.
98. K. A. Holbrook, M. J. Pilling, and S. H. Robertson, *Unimolecular Reactions*, Wiley, Chichester, 2nd edn., 1996.
99. J. W. Davies and M. J. Pilling, in *Advances in Gas Phase Photochemistry and Kinetics*, Eds M. N. R. Ashfold and J. E. Baggott, Royal Society of Chemistry, London, 1989, vol. 2, Chapt. 3, p. 105.
100. U. N. Alexander, K. D. King, and W. D. Lawrance, *Phys. Chem. Chem. Phys.*, 2003, **5**, 1557.
101. U. N. Alexander, K. D. King, and W. D. Lawrance, *J. Phys. Chem. A*, 2002, **106**, 973.
102. R. Becerra, J. P. Cannady, and R. Walsh, *J. Phys. Chem. A*, 2003, **107**, 11049.
103. M. W. Heaven, G. F. Metha, and M. A. Buntine, *Aust. J. Chem.*, 2001, **54**, 185.
104. R. Becerra, I. W. Carpenter, G. J. Gutsche, K. D. King, W. D. Lawrance, W. S. Staker, and R. Walsh, *Chem. Phys. Lett.*, 2001, **333**, 83.
105. S. R. Gunn and L. G. Green, *J. Phys. Chem.*, 1961, **65**, 779.
106. S. R. Gunn and J. H. Kindsvater, *J. Phys. Chem.*, 1966, **70**, 1750.
107. M. J. Almond, A. M. Doncaster, P. N. Noble, and R. Walsh, *J. Am. Chem. Soc.*, 1982, **104**, 4717.
108. P. N. Noble and R. Walsh, *Int. J. Chem. Kinet.*, 1983, **15**, 547.
109. B. Ruscic, M. Schwartz, and J. Berkowitz, *J. Chem. Phys.*, 1990, **92**, 1865.

110. W. E. Dasent, *Nonexistent Compounds*, Arnold, London, 1965, Chapt. 5, p. 77.
111. S. W. Benson, *Thermochemical Kinetics*, Wiley, New York, 2nd edn., 1976.
112. J. A. Boatz and M. S. Gordon, *J. Phys. Chem.*, 1989, **93**, 3025.
113. J. A. Boatz, M. S. Gordon, and L. R. Sita, *J. Phys. Chem.*, 1990, **94**, 5488.
114. A. M. Doncaster and R. Walsh, *J. Phys. Chem.*, 1979, **83**, 578.
115. L. H. Long and C. I. Pulford, *J. Chem. Soc., Faraday Trans.*, 1986, **82**, 567.
116. R. Becerra, S. E. Boganov, M. P. Egorov, V. I. Faustov, I. V. Krylova, O. M. Nefedov, and R. Walsh, *J. Am. Chem. Soc.*, 2002, **124**, 7555.
117. L. R. Sita and R. D. Bickerstaff, *Phosphorus, Sulfur Silicon Relat. Elem.*, 1989, **41**, 31.
118. J. P. Cotton, P. J. Davidson, M. F. Lappert, *J. Chem. Soc., Dalton Trans.*, 1976, 2275.
119. U. N. Alexander, *Ph. D. Thesis*, Flinders University of South Australia, 2000.

Received October 7, 2004;
in revised form March 2, 2005